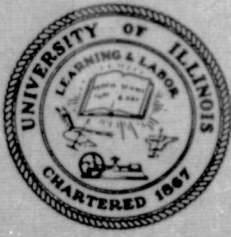


## General Disclaimer

### One or more of the Following Statements may affect this Document

- This document has been reproduced from the best copy furnished by the organizational source. It is being released in the interest of making available as much information as possible.
- This document may contain data, which exceeds the sheet parameters. It was furnished in this condition by the organizational source and is the best copy available.
- This document may contain tone-on-tone or color graphs, charts and/or pictures, which have been reproduced in black and white.
- This document is paginated as submitted by the original source.
- Portions of this document are not fully legible due to the historical nature of some of the material. However, it is the best reproduction available from the original submission.



UNIVERSITY OF ILLINOIS  
URBANA

# AERONOMY REPORT NO. 33

## FULL-WAVE CALCULATIONS OF REFLECTION COEFFICIENTS FROM D-REGION ELECTRON-DENSITY PROFILES

by  
W. A. Viertel  
C. F. Sechrist, Jr.

June 1, 1969

FACILITY FORM 602	<u>N69-35646</u> (ACCESSION NUMBER)	_____
	<u>73</u> (PAGES)	<u>1</u> (THRU)
	<u>CR-105425</u> (NASA CR OR TMX OR AD NUMBER)	_____
		<u>13</u> (CODE)
		_____
		(CATEGORY)

Supported by  
National Aeronautics and Space Administration  
Grant ~~NGR-013~~ NGR-14-005-013

Aeronomy Laboratory  
Department of Electrical Engineering  
University of Illinois  
Urbana, Illinois

#### CITATION POLICY

The material contained in this report is preliminary information circulated rapidly in the interest of prompt interchange of scientific information and may be later revised on publication in accepted aeronomic journals. It would therefore be appreciated if persons wishing to cite work contained herein would first contact the authors to ascertain if the relevant material is part of a paper published or in process.

A E R O N O M Y   R E P O R T

N O.   3 3

FULL-WAVE CALCULATION  
OF REFLECTION COEFFICIENTS  
FROM D-REGION ELECTRON-DENSITY PROFILES

by

W. A. Viertel  
C. F. Sechrist, Jr.

June 1, 1969

Supported by  
National Aeronautics and  
Space Administration  
Grant ~~NGR-013~~ NGR-14-005-013

Aeronomy Laboratory  
Department of Electrical Engineering  
University of Illinois  
Urbana, Illinois

## ABSTRACT

This report considers the reflection of VLF radio waves from the D-region of the ionosphere. In particular, the calculation of the reflection coefficient matrix below the ionosphere is described. Full-wave theory is employed in a FORTRAN IV computer program for use with the IBM 360 computer. The program is checked by comparing computed reflection coefficients with those obtained by an analytical method for the case of a vertical geomagnetic field and an exponential electron density model, and also with full-wave computations done by other groups for a more general case. The report concludes with suggestions for the application of the full-wave program to the computation of VLF reflection coefficients from D-region electron density profiles measured by ground-based and rocket techniques.

TABLE OF CONTENTS

	Page
ABSTRACT. . . . .	.iii
LIST OF FIGURES . . . . .	.vi
LIST OF TABLES. . . . .	.viii
1. THE D REGION OF THE IONOSPHERE. . . . .	1
1.1 Introduction . . . . .	1
1.2 VLF Studies of the D Region. . . . .	6
2. RAY THEORY. . . . .	9
2.1 The Theory of Booker . . . . .	9
2.2 The Necessity for Full-Wave Theory . . . . .	17
3. FULL-WAVE THEORY. . . . .	18
3.1 General Magnetoionic Theory. . . . .	18
3.2 The Relevant Equations . . . . .	26
4. FULL-WAVE SOLUTIONS . . . . .	30
4.1 The Starting Solution. . . . .	30
4.2 The Numerical Integration. . . . .	31
4.3 Checks of the Full-Wave Program. . . . .	39
4.4 Suggestions for Applications of the Full-Wave Program. . . . .	45
APPENDIX. . . . .	49
REFERENCES. . . . .	65

## LIST OF FIGURES

Figure		Page
1.1	The F-region (after Farley, 1966), E-region (after Monro and Bowhill, 1969), and D-region (after Mechtly and Smith, 1968) of the ionosphere. . . . .	2
1.2	Electron collision frequency profiles (after Deeks, 1964). . . . .	5
1.3	Components of the field at the ground (after Bracewell, 1952). . . . .	7
2.1	A ray path for a wave-packet incident obliquely upon an inhomogeneous, isotropic, collisionless ionosphere (after Booker, 1938). . . . .	10
2.2	Group- and phase-rays of the (a) extraordinary wave, and the (b) ordinary wave, for an inhomogeneous, anisotropic, collisionless ionosphere (after Booker, 1938) . . . . .	12
2.3	The Booker quartic roots $q$ as a function of electron density $N$ , for oblique incidence upon an inhomogeneous, anisotropic ionosphere (after Booker, 1938). The dashed curve represents the extraordinary wave; the solid curve represents the ordinary wave . . . . .	14
2.4	Another possible form of (a) $q$ as a function of $N$ for oblique incidence upon an inhomogeneous, anisotropic ionosphere with collisions included, and (b) the corresponding group-ray diagram (after Booker, 1938) . . . . .	16
3.1	Height variation of $\nu_M$ the collision frequency of monoenergetic electrons of energy $kT$ (full curve) and $\nu_{eff}$ , the effective classical collision frequency for very long wave calculations (dashed curve), (after Deeks, 1966a). . . . .	22
3.2	The relevant coordinate system at the transmitter. The wave vector $\bar{k}$ is in the $xz$ plane. $\bar{B}$ is in the plane of the magnetic meridian. $\beta, \gamma, \Delta$ are the arccosines of the direction cosines $l, m, n$ of the geomagnetic field vector, $\bar{Y}$ . . . . .	25
4.1	Flow chart depicting (a) input portion of main program, including (b) subroutine PREFN . . . . .	32
4.2	Flow chart depicting initial solution (after Sheddy, 1968) portion of main program. . . . .	33
4.3	Flow chart depicting numerical integration subroutine DRKGS. . . . .	37

## LIST OF FIGURES (Continued)

Figure	Page
4.4	Flow chart depicting subroutines (a) FCT and (b) OUTP called from within DRKGS subroutine. . . . . 38
4.5	Flow chart depicting final output portion of main program. . . . 40
4.6	A comparison of the full-wave results, reflection coefficient magnitude vs angle of incidence, for $\nu$ constant, $\phi = 90^\circ$ , and $\alpha = 90^\circ$ , of (a) Budden (1955b) (solid line), Budden using the formulas of Heading and Whipple (1952) (dashed line), and the author (points marked x) for $X = \exp(.295z)$ , $Z = 8$ and (b) Budden (1955b) (solid line) and the author (points marked x) for $X = \exp(2.36z)$ , $Z = 2$ . . . . . 44
4.7	D-region electron density profiles for night, dawn, and day-time periods (after Smith <u>et al.</u> , 1966) deduced from ground-based measurements . . . . . 46
4.8	D-region electron density profiles over the sunrise period measured with rockets (after Mechtly and Smith, 1968). . . . . 47



## LIST OF TABLES

Table		Page
4.1	A comparison of the author's numerically calculated starting solutions with those of Fedor, <u>et al.</u> , (1964) of NELC. . . . .	42
4.2	A comparison of full-wave solutions for the nighttime electron density profile of Deeks (1964) and the collision frequency profile of Fejer and Vice (1959) . . . . .	43

## 1. THE D REGION OF THE IONOSPHERE

### 1.1 Introduction

The D region of the ionosphere is the region between 60 and 90 km, coinciding roughly with the mesosphere and lower thermosphere. A daytime profile showing its place in the entire ionosphere is shown in Figure 1.1. The F region and the topside of the ionosphere are from the observation of the equatorial ionosphere of Farley (1966), who used the incoherent backscatter technique to measure them. The E region portion of the profile was obtained from Nike-Apache rocket measurements at Wallops Island, Virginia, and is from Monro and Bowhill (1969). The D region representation, measured in the same way as the E region, is due to Mechtly and Smith (1968). The entire profile will vary with latitude, longitude, solar zenith angle, season, the solar cycle, and the instantaneous level of solar disturbances.

At sunset with the disappearance of the ionizing solar radiation, the D region electron density drops markedly. At dawn the number of free electrons at any given height gradually returns to its daytime value. The exact shape of the profiles is not universally agreed upon, however, as shown in the comparison made by Deeks (1964). Some show a minimum followed by a maximum at lower altitude in the daytime profile, while others show a more monotonically decreasing electron density with decreasing altitude, apart from some slight fine structure. It may be that when the time and place, as well as the manner of measurement or deduction, are all taken into account and D region theory is better understood, these profiles will be shown to be generally consistent with one another. The difficulty in understanding the D region stems

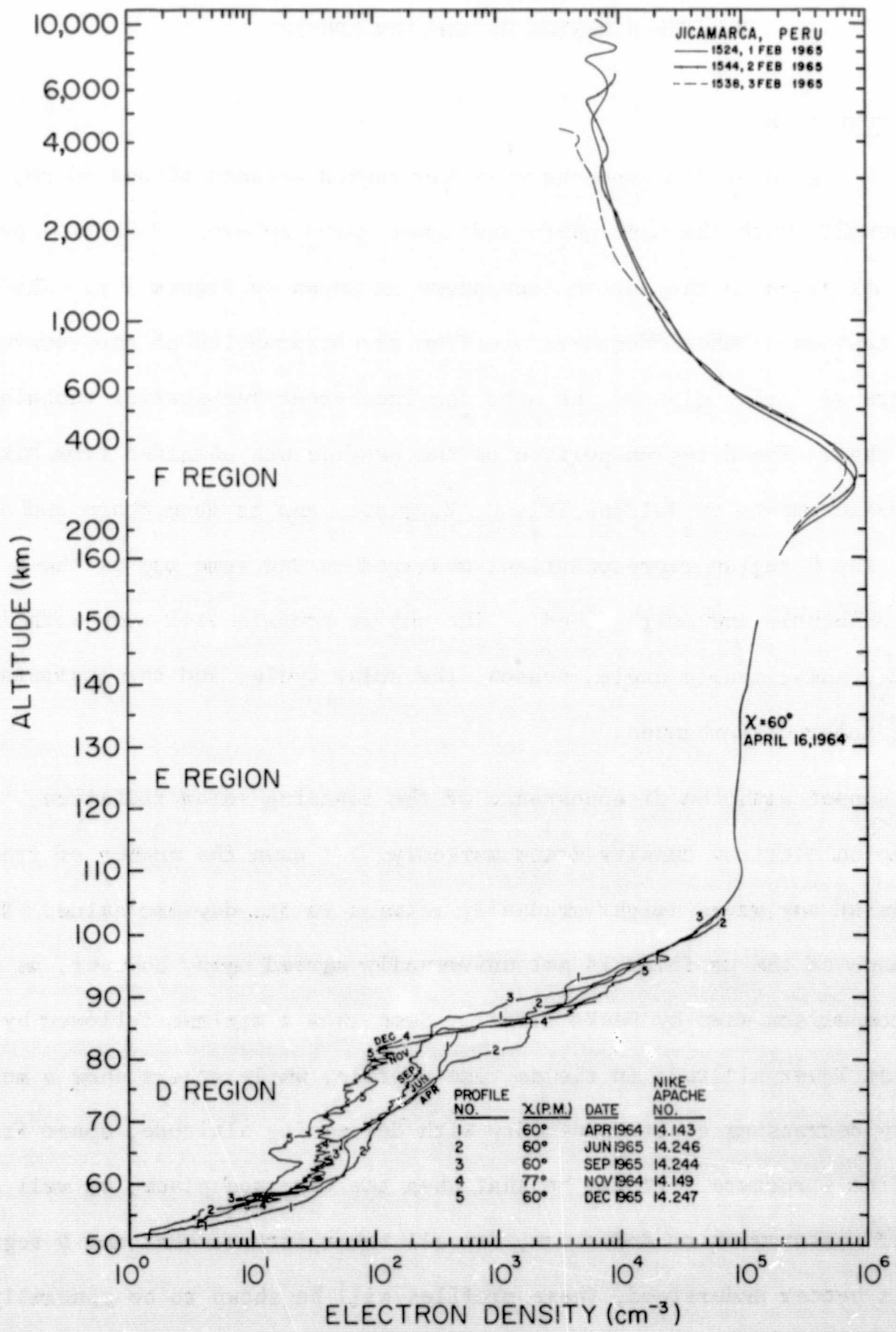


Figure 1.1 The F-region (after Farley, 1966), E-region (after Monro and Bowhill, 1969), and D-region (after Mechtly and Smith, 1968) of the ionosphere.

from its relative inaccessibility to measurements, having an atmospheric concentration too low for aircraft and too high for satellites. Thus rockets and ground-based equipment are the chief tools for studying the D region.

Several types of radiation are thought to be important causes of ionization in the D region. Solar radiations penetrating below 85 km, given by Nicolet and Aikin (1960), are X-rays of  $\lambda < 10 \text{ \AA}$ , Lyman  $\alpha$  ( $\lambda = 1215.7 \text{ \AA}$ ) and radiation in other nearby atmospheric windows, and radiation of  $\lambda > 1800 \text{ \AA}$ . The X-rays and ultraviolet radiation (Lyman  $\beta$  and the Lyman continuum) are probably important above 85 km during periods of normal solar activity, while an enhanced X-ray flux may affect all constituents, chiefly  $O_2$ ,  $N_2$ , A and O at lower D region heights during solar flares. NO is one of the few species having a sufficiently low ionization potential to be ionized by Lyman  $\alpha$ . The importance of the ionization of NO by Lyman  $\alpha$  relative to the ionization of other constituents by other radiations depends upon the quantities of NO assumed to be present as is shown by Aikin, et al., (1964). In any case, it seems to be most important in the region around 77 km. Radiations of  $\lambda > 1800 \text{ \AA}$  require constituents with very low ionization potentials, such as calcium ( $\lambda \leq 2028 \text{ \AA}$ ) and sodium ( $\lambda \leq 2413 \text{ \AA}$ ).

Below the region where ionization of NO is important, galactic and solar cosmic rays are thought to be the principal causes of ionization, although their contribution to the number of free electrons is tempered at these lower D region altitudes by the importance of negative ions due to attachment. The relative importance of contributions to ionization by protons,  $\alpha$ -particles, and H-nucleii is treated by Velinov (1968).

Recently metastable  $O_2(^1\Delta)$  has been suggested by Hunten and McElroy (1963) as a significant source of ionization in the D region. It can be ionized by

the wavelength band 1027-1118 Å, some of which penetrates to the D region through atmospheric windows. In addition, the reaction of this excited  $O_2$  with N may be the most important source of nitric oxide in the D region.

Corpuscular radiation in the form of electrons with energy greater than 40 kev precipitating from the radiation "belts" has also been suggested as an important ionization source at D region altitudes by Tulinov (1967). Further discussion of the chemical and meteorological factors affecting D region free electron concentrations may be found in the record of the Third Aeronomy Conference held at the University of Illinois, September 23-26, 1968.

Another relevant factor is the collisions between electrons and neutral constituents. Electron-electron and electron-ion collisions are not so important because of the far greater number of neutrals present. The altitude dependence of collision frequency given by many workers and compiled by Deeks (1964) is shown for the D region in Figure 1.2. Belrose and Bourne (1966) conclude that the greatest seasonal change in collision frequency occurs at high latitudes. They state that no diurnal changes have been detected, but more measurements are necessary to determine the dependence of collision frequency on the solar cycle and solar disturbances. The relevance of this parameter, along with the electron density, is that it affects radio waves propagating through the ionosphere.

The major objective of this thesis is to devise a computer program for use with the IBM 360 digital computer to calculate the theoretical reflection and conversion coefficients for a VLF radio wave obliquely incident upon the ionosphere. The theory for the ionospheric model and for the model of the wave-ionosphere interaction chosen is discussed in detail.

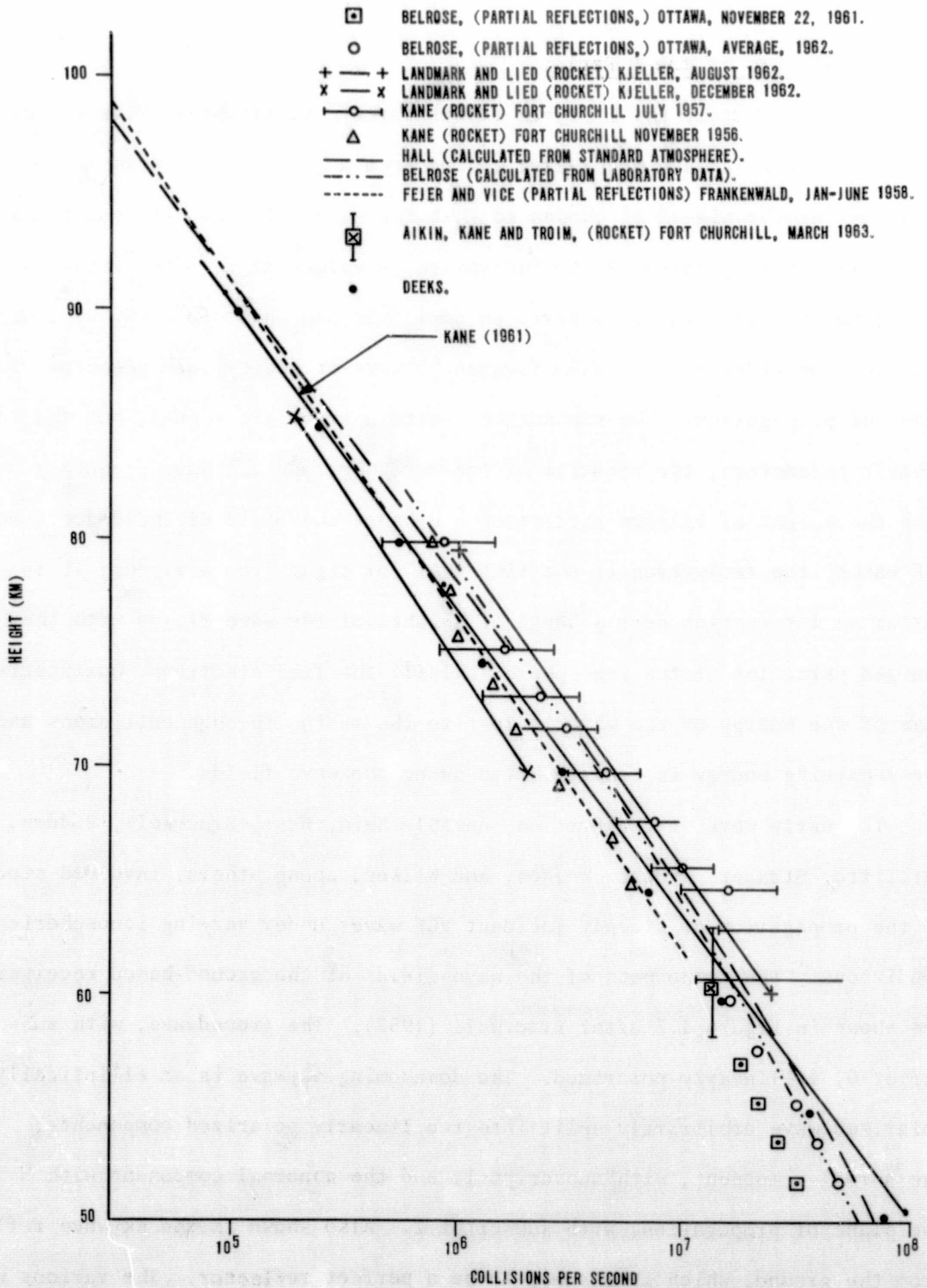


Figure 1.2 Electron collision frequency profiles (after Deeks, 1964).

## 1.2 VLF Studies of the D Region

One way to study the D region experimentally is to observe its effect on an electromagnetic wave propagated upward from a ground-based transmitter. The frequency of the signal is chosen so that the wave will have its maximum interaction with that portion of the ionosphere in which one is interested. A receiver detects the signal, altered in amplitude and phase in a way dependent upon the electron density, collision frequency, wave-frequency, and geometry of the plane of propagation. The transmitter emits a symmetric signal, but the ionospheric parameters, the location of the receiver, and the wave-frequency determine the height of maximum reflection and hence the angle of incidence. For VLF waves, the reflection is not like that for light from a mirror; it is rather an interaction over a range of heights of the wave fields with the charged particles of the ionosphere, chiefly the free electrons. Qualitatively, some of the energy of the wave is lost to the medium through collisions and the remaining energy is redistributed among the wave fields.

The early work of the British, notably Bain, Best, Bracewell, Budden, Ratcliffe, Straker, Stuart, Weekes, and Wilkes, among others, involved studies of the propagation of steeply incident VLF waves under varying ionospheric conditions. The components of the wave-fields at the ground-based receiver are shown in Figure 1.3 after Bracewell (1952). The groundwave, with subscript 0, is linearly polarized. The downcoming skywave is an elliptically polarized wave arbitrarily split into two linearly polarized components, the normal component, with subscript 1, and the abnormal component with  $\bar{H}$  in the plane of propagation, with subscript 2. Also shown is the skywave reflecting from the ground, which is assumed to be a perfect reflector. The various wave-fields making up the total magnetic field at the ground are shown in Figure 1.3B.

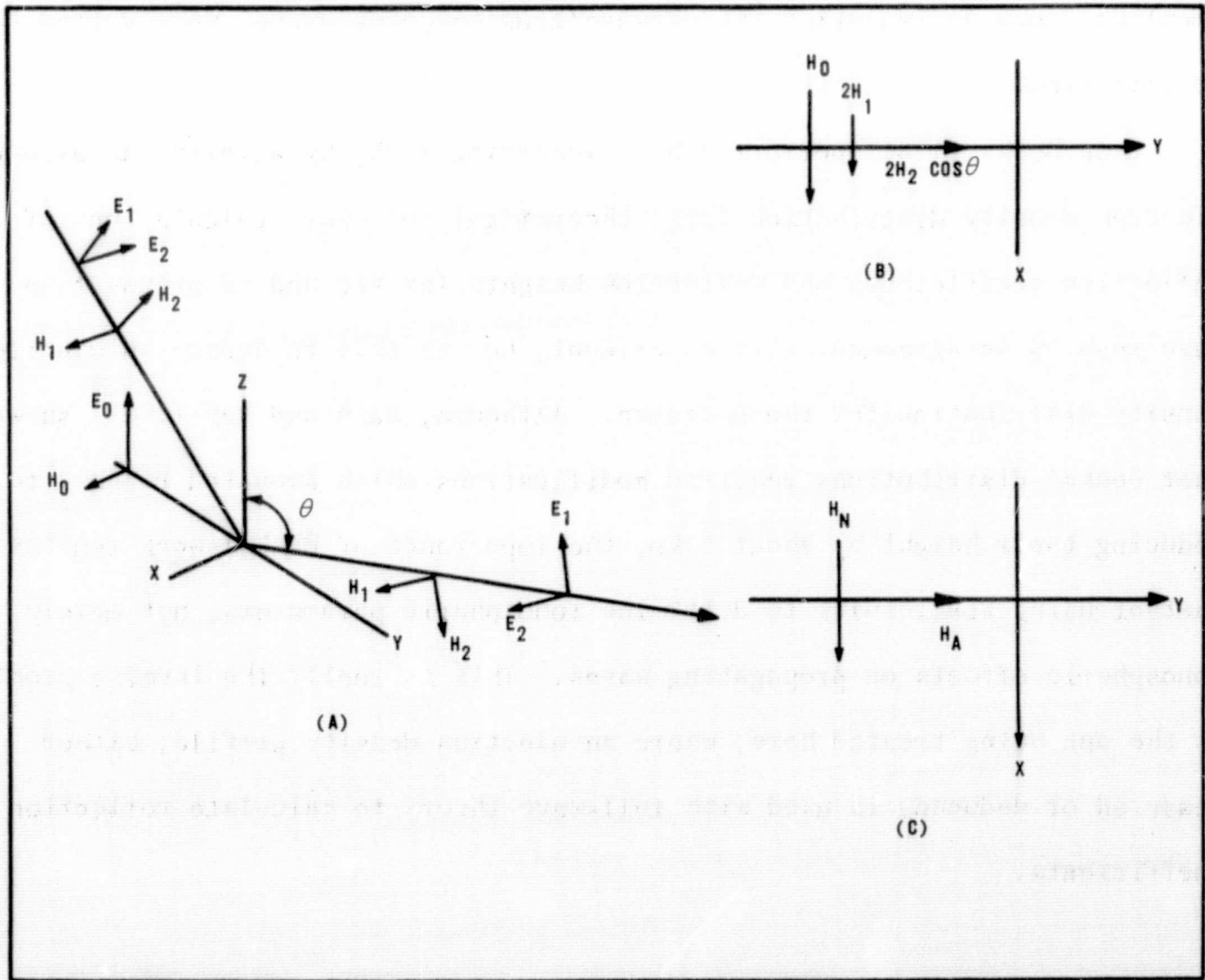


Figure 1.3 Components of the field at the ground (after Bracewell, 1952).



Figure 1.3C depicts the measurable quantities  $H_N$ , the total normal component, and  $H_A$ , the total abnormal component, the two vectors in general being out of phase. Basically, this work was a cataloging of the ionosphere's effect on this received signal as a function of time and space. Various experimental problems, such as isolating the skywave from the groundwave, were worked out at this time.

Then Deeks (1966) performed his pioneering work; by altering an assumed electron density distribution until theoretical full-wave calculations of reflection coefficients and reflection heights for VLF and LF propagation gave results in agreement with experiment, he was able to deduce an electron density distribution for the D region. Although, Bain and May (1967) showed that Deeks' distributions required modifications which amounted roughly to reducing their height by about 6 km, the importance of Deeks' work remains, that of using VLF results to determine ionospheric parameters, not merely ionospheric effects on propagating waves. This is really the inverse problem to the one being treated here, where an electron density profile, either measured or deduced, is used with full-wave theory to calculate reflection coefficients.

## 2. RAY THEORY

### 2.1 The Theory of Booker

Historically, ray theory preceded full-wave theory. According to the ray theory, a wave incident on the ionosphere from below with an angle of incidence  $\theta$  measured from the vertical may be thought of as a ray, much as one thinks of light rays in geometrical optics. For simple situations, such as no magnetic field and no electron-neutral collisions, the path of the ray may be traced through the atmosphere by following the phase velocity vector. The orientation of this vector changes along the path through the ionosphere according to Snell's Law

$$\mu \sin \psi = \sin \theta \quad , \quad (2.1)$$

where  $\mu$  is the phase refractive index and  $\psi$  is the angle the phase velocity makes with the vertical. Below the region of ionization in the atmosphere,  $\mu = 1$ . In the inhomogeneous, isotropic, collisionless ionosphere above this free space region,  $\mu$  decreases with increasing altitude. When the level is reached where  $\psi = \frac{\pi}{2}$ , the wave has achieved its deepest penetration into the ionosphere, and it then begins its descent. The ray path for such a simple situation is shown in Figure 2.1. Line AB is the boundary between the free space region and the region of ionization.

Booker (1938) pointed out that the inclusion of the earth's magnetic field makes the situation much more complicated. Upon entering the ionosphere, the incident wave may be thought of as being split into two characteristically polarized components, which may propagate independently. The refractive index is now dependent upon  $\psi$ , as well as altitude, in a complicated way, and Snell's

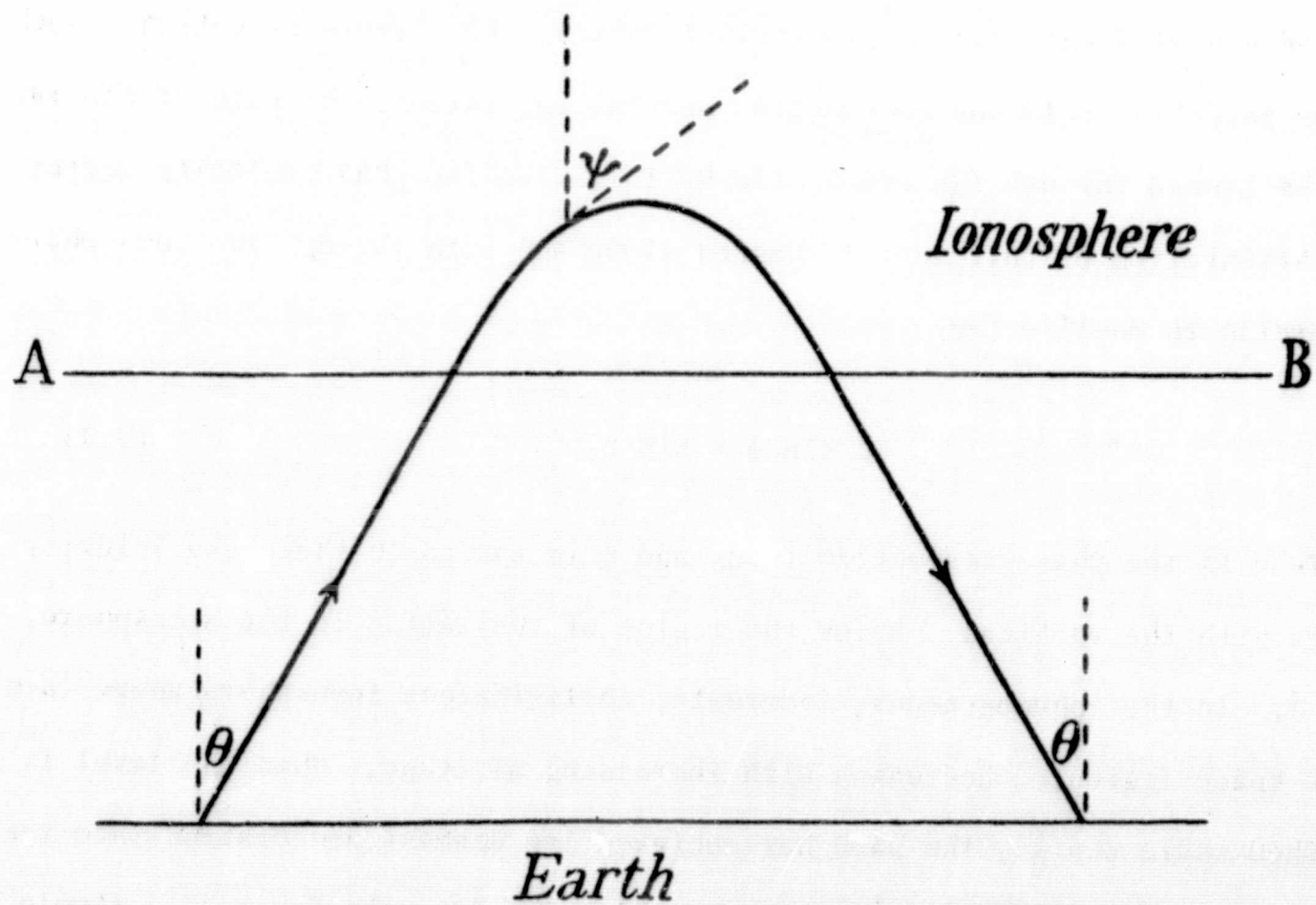


Figure 2.1 A ray path for a wave-packet incident obliquely upon an inhomogeneous, isotropic, collisionless ionosphere (after Booker, 1938).

Law with  $\psi = \frac{\pi}{2}$  will no longer give the level of reflection of the wave. The level where the group velocity, not the phase velocity, is horizontal is the true level of reflection. This level was the same for the case of no magnetic field because the group and phase velocity vectors were identical. As a wave-packet propagates through the region of ionization with the group velocity, the individual wave-crests within it are in general moving across the wave-packet with a phase velocity of different magnitude and direction from the group velocity. This results in a cusped ray path for each of the two magnetoionic components, the ordinary and extraordinary waves. These paths are shown in Figure 2.2 along with the corresponding group-rays. The figure shows only the behavior in the xz plane. Thus the phase-rays do not actually show the path followed by the wave-packet, but only the direction at any altitude of the wave-crests moving across the wave-packet. This is also shown in Figure 2.2 by superimposing phase velocity vectors on the group-ray path.

Because of the dependence of  $\mu$  on the unknown angle of refraction  $\psi$ , it proves convenient to approach the problem of obliquely incident propagation by avoiding the use of  $\mu$ . The propagation of either of the two magnetoionic components is represented by the wave function

$$\exp [ik \{ct - \mu(\psi)((\sin \psi)x + (\cos \psi)z)\}] \quad (2.2)$$

Using Snell's Law and a newly defined variable  $q$ , the wave function becomes

$$\exp [ik \{ct - (\sin \theta)x - qz\}] \quad (2.3)$$

where  $q$  is the only unknown.  $q$  contains the electron density, wave-frequency, earth's magnetic field, and angle of incidence as parameters, and the

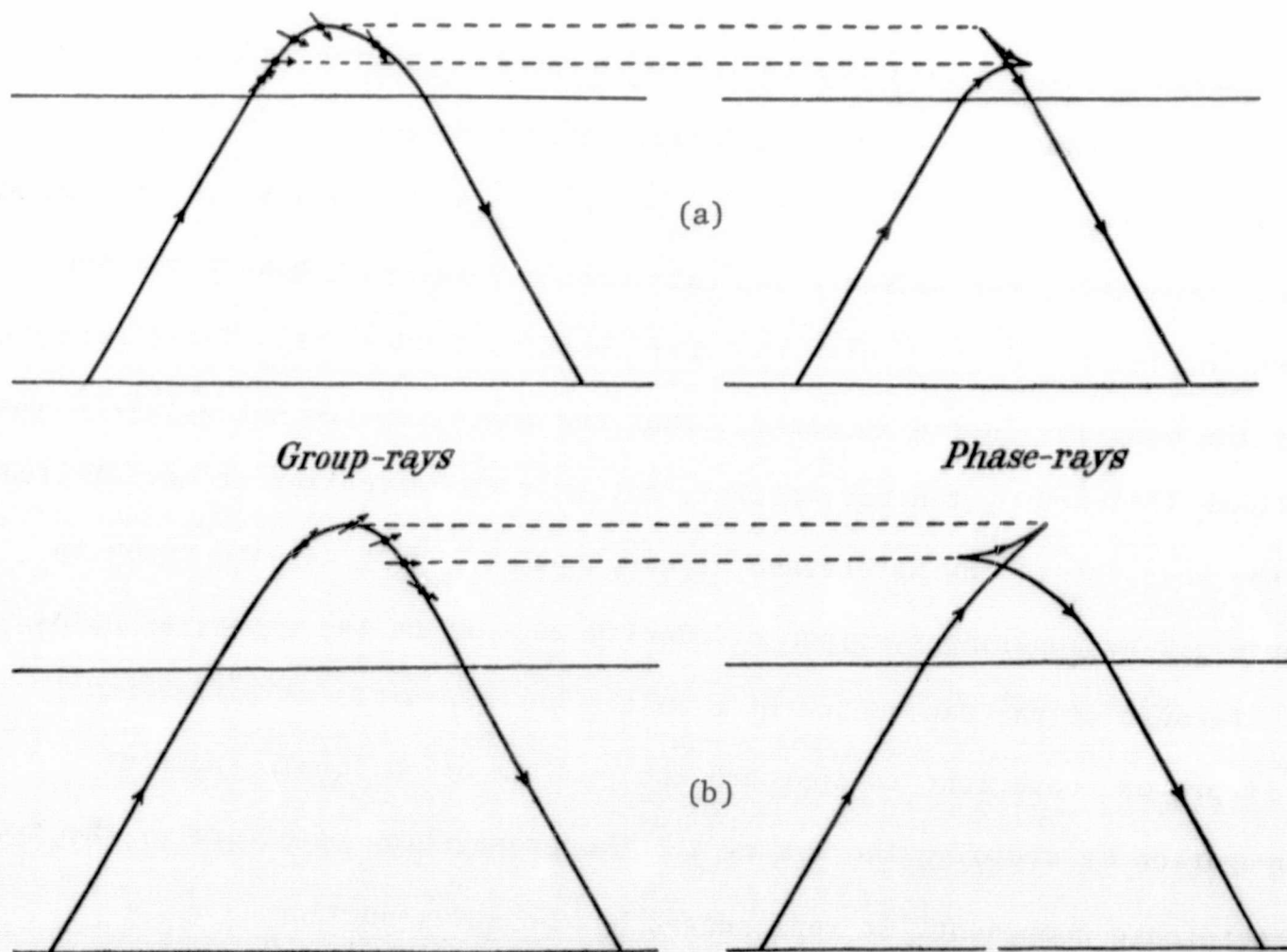


Figure 2.2 Group- and phase-rays of the (a) extraordinary wave, and the (b) ordinary wave, for an inhomogeneous, anisotropic, collisionless ionosphere (after Booker, 1938)

propagation of the wave components through the atmosphere can now be represented by plotting  $q$  as a function of the electron density  $N$  while keeping the other three parameters constant. Such a plot is shown in Figure 2.3. It would be symmetrical for vertical incidence. Below the ionosphere  $N = 0$  and  $q = \cos \theta$ . There is a critical electron density ( $N_A$  or  $N_B$  in Figure 2.3) for each magnetoionic component, above which that component will not penetrate for a given wave-frequency and angle of incidence. Hence the reflection points (A and B in Figure 2.3) are represented by  $\frac{\partial q}{\partial N} \rightarrow \infty$ , not  $\psi = \frac{\pi}{2}$  or  $q = 0$  (D and E in Figure 2.3) as was the case for the isotropic ionosphere.

Following the example of Appleton, whose wave-function one may retrieve from Booker's by letting  $\theta = 0$ , the wave function, which was the assumed form of the electromagnetic wave-fields and the polarization, was substituted into the wave equations obtained from Maxwell's equations, resulting in a quartic equation in  $q$ , instead of the quadratic obtained by Appleton, represented by

$$F(q) \equiv \alpha q^4 + \beta q^3 + \gamma q^2 + \delta q + \epsilon = 0 \quad . \quad (2.4)$$

The four Booker quartic roots correspond to the upgoing ordinary, downgoing ordinary, upgoing extraordinary, and downgoing extraordinary waves. The exact nature of the coefficients in the Booker quartic equation depends on the assumptions concerning electron-neutral collisions and the form of the constitutive relation between the polarization  $\bar{P}$  and the electric field intensity  $\bar{E}$ . If the collisional damping due to electron-neutral collisions is included, the coefficients of the Booker quartic equation and the Booker quartic roots become complex quantities.

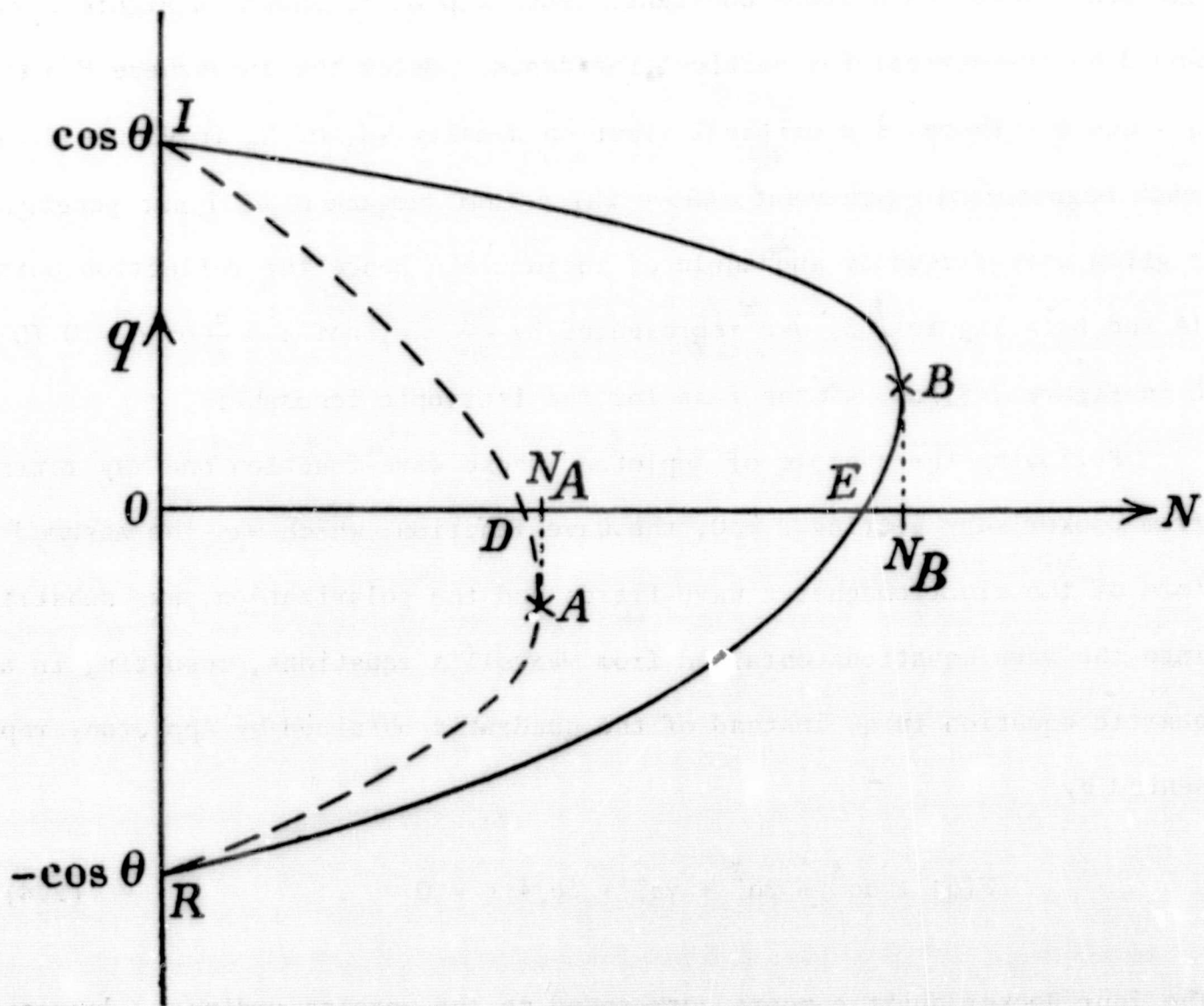


Figure 2.3 The Booker quartic roots  $q$  as a function of electron density  $N$ , for oblique incidence upon an inhomogeneous, anisotropic ionosphere (after Booker, 1938). The dashed curve represents the extraordinary wave; the solid curve, represents the ordinary wave.

The quartic equation may be solved at any altitude, even for complex coefficients, by the method of Burnside and Panton (1904). Figure 2.3 may thus be obtained if the variation of electron density with height, the wave-frequency, the angle of incidence at the ground, and the earth's magnetic field vector, which is assumed to remain constant in magnitude and direction over the region of propagation, are specified.

The wave-fields for the upgoing extraordinary wave, downcoming extraordinary wave, upgoing ordinary wave, and downcoming ordinary wave are proportional at any altitude to

$$\exp \{ ik (ct - (\sin \theta)y - \int_0^z q dz) \} , \quad (2.5)$$

where the root  $q$  used is the one appropriate to the magnetoionic component under consideration. Since the form of the relationship between  $q$  and  $z$  or  $N$  can be very complicated, the integration in (2.5) may have to be performed numerically. The real part of  $q$  determines the phase change in the wave, whereas the imaginary part arising from collisional damping determines the attenuation as the integration proceeds. The integration for each magnetoionic component might also involve several separate parts due to a situation such as the one shown in Figure 2.4, where a  $q$  vs  $N$  plot and the corresponding group-ray diagram are depicted. The upgoing ordinary wave is represented by IB and  $A_2A_3$ , the downgoing ordinary wave by RB and  $A_2A_1$ , the upgoing extraordinary wave by  $IA_1$ , and the downgoing extraordinary wave by  $RA_3$ .

In any case, the reflection coefficients could in principle be calculated by comparing the wave-fields at the end of the path with those at the start



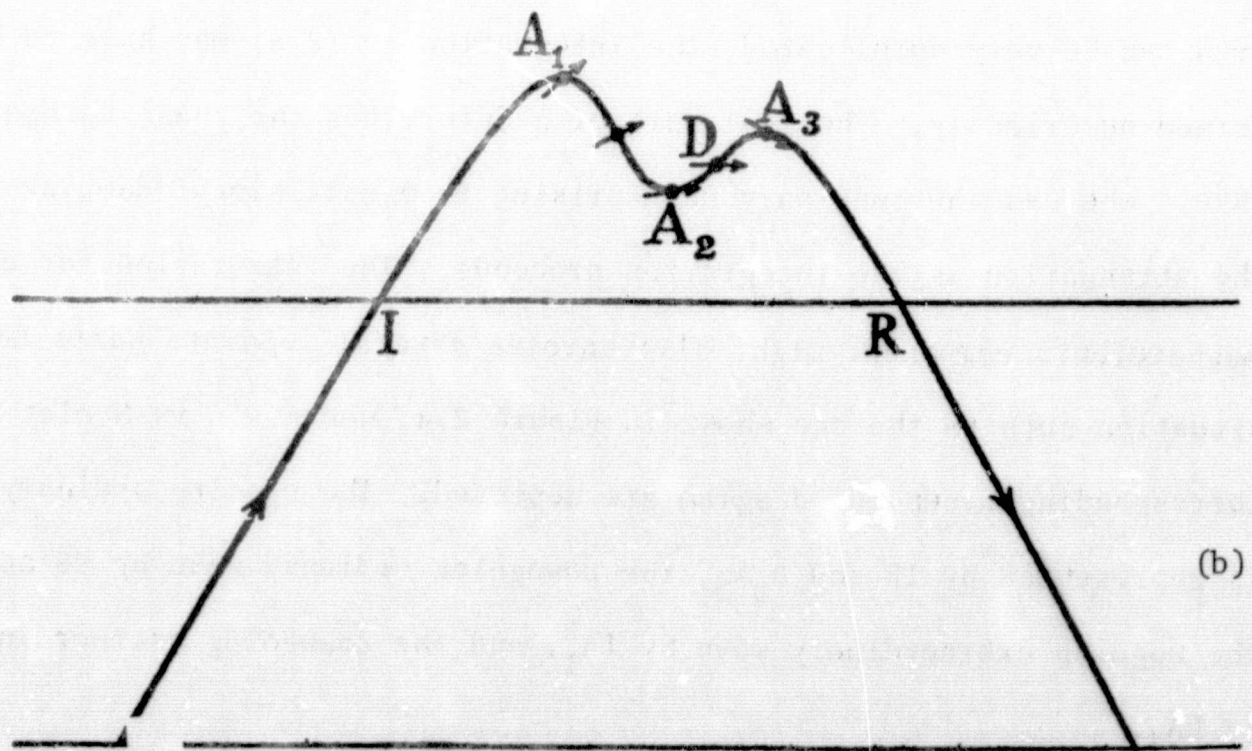
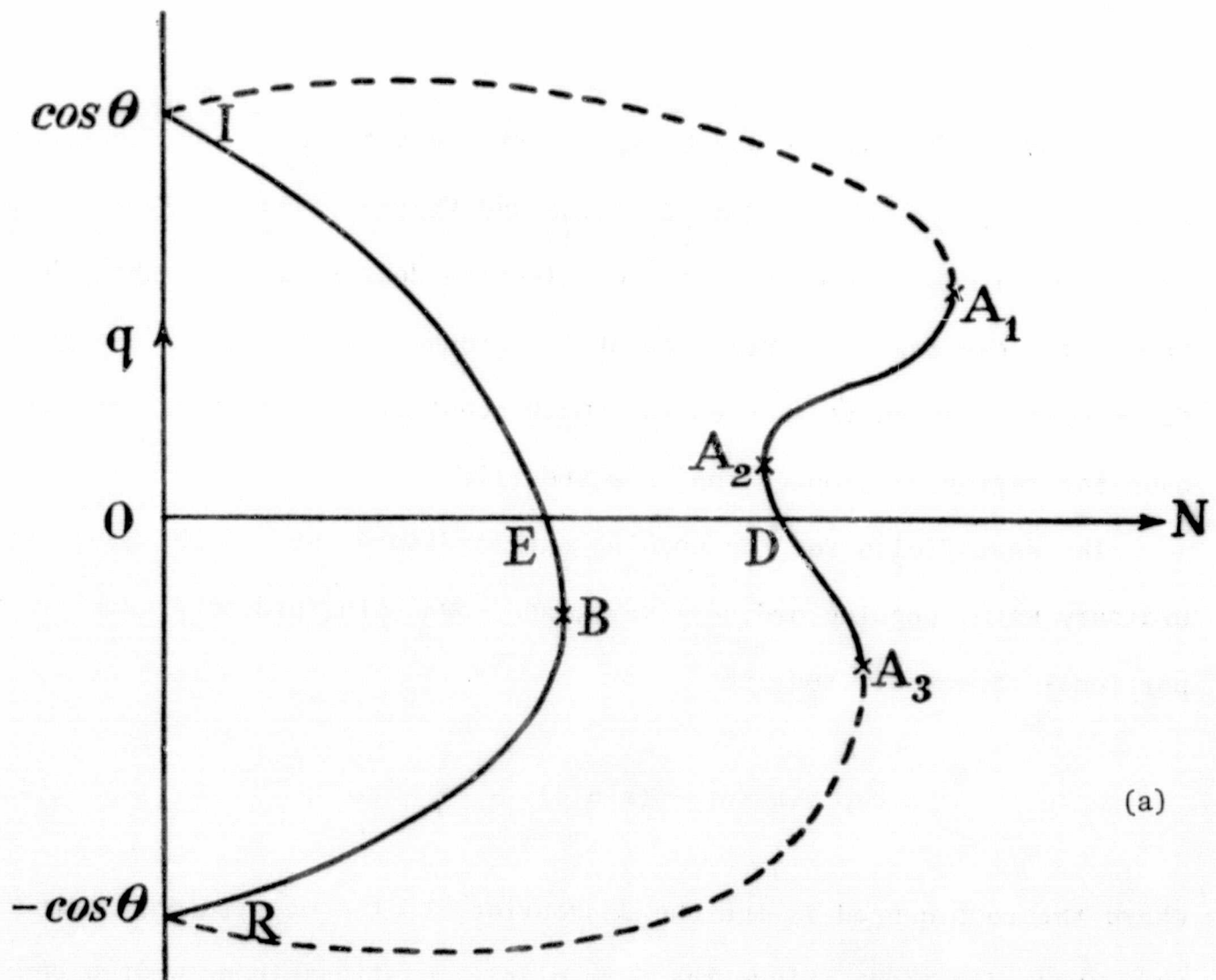


Figure 2.4 Another possible form of (a)  $q$  as a function of  $N$  for oblique incidence upon an inhomogeneous, anisotropic ionosphere with collisions included, and (b) the corresponding group-ray diagram (after Booker, 1938).

after all the phase change and attenuation, which occur over the whole path, and all the absorption, which occurs only over the portion of the path in the ionosphere, have altered the wave.

## 2.2 The Necessity for Full Wave-Theory

A wide variety of situations exist for which the ray theory is invalid; it fails to give a good description of reality. Booker (1938) discusses the failure of the theory in the stratum in which reflection takes place, that is, when the quartic roots for the upgoing and downgoing waves of either the ordinary (or extraordinary) component become nearly equal. He also mentions the failure in a region of coupling when the upgoing (or downgoing) waves of the ordinary and extraordinary component become nearly equal, and the two components thus lose their independence. Failure also occurs when the collisional damping is so great that reflection cannot be considered to occur at one height alone, but occurs partially at different levels. The failure of the medium to be slowly varying at the wave-frequency being used is the common factor in all of the inadequacies of ray theory. Usually, below wave-frequencies of 1 MHz, and always below wave-frequencies of 100 KHz, one must resort to a more exact solution of the electromagnetic wave equations. The form of the wave-fields assumed by Booker is no longer valid. The refractive indices of the ionosphere change appreciably within one wavelength. The upgoing energy is converted by the ionosphere to downgoing energy over a range of heights. Since studies of the D region involve frequencies of a few tens of KHz, it is necessary to employ the more exact full-wave theory.

### 3. FULL-WAVE THEORY

#### 3.1 General Magnetoionic Theory

To develop a mathematical formalism to describe waves obliquely incident upon a horizontally stratified anisotropic, collisional, non-thermal, non-slowly varying, non-permeable ( $\mu = \mu_0$ ), inhomogeneous ionosphere, one must first begin with the equation for conservation of charge, the continuity equation

$$m_\alpha \frac{\partial N_\alpha}{\partial t} + m_\alpha \bar{\nabla} \cdot (N_\alpha \bar{v}_\alpha) = 0 \quad ; \quad (3.1)$$

and the force equation, the magnetohydrodynamic equation

$$m_\alpha \frac{D\bar{v}_\alpha}{Dt} = z_\alpha e \bar{E} + z_\alpha e \bar{v}_\alpha \times \bar{B} + m_\alpha N_\alpha \bar{g} - \frac{\bar{\nabla} p}{N_\alpha} - m_\alpha \nu_\alpha \bar{v}_\alpha \quad , \quad (3.2)$$

where the subscript  $\alpha$  indicates a summation over the  $\alpha$  charged constituents and the  $D/Dt$  is the convective derivative

$$\frac{D}{Dt} = \frac{\partial}{\partial t} + \bar{v}_\alpha \cdot \bar{\nabla} \quad , \quad (3.3)$$

which in this case gives the total time rate of change of the  $\alpha$ th constituent's velocity,  $\bar{v}_\alpha$ , on the left hand side of the force equation. Other quantities appearing in Equations (3.1) and (3.2) are the mass of the  $\alpha$ th charged constituent,  $m_\alpha$ ; the number density of the  $\alpha$ th charged constituent,  $N_\alpha$ ; the electric field of the skywave,  $\bar{E}$ ; the total magnetic field, including the earth's magnetic field and the magnetic field of the skywave,  $\bar{B}$ ; the gravitational acceleration field,  $\bar{g}$ ; the scalar fluid pressure of the plasma,  $p$ ; and the collision frequency, measured in collisions per second, of the

$\alpha$ th charged constituent with ions, electrons, and neutral atoms and molecules,  $v_{\alpha}$ . The definition of these quantities makes the nature of each of the force terms on the righthand side of Equation (3.2) self-explanatory.

If it was desired to examine the propagation in the plasma in terms of characteristic modes, one would form perturbed equations using

$$N_{\alpha} = N_{\alpha 0} + N_{\alpha}'$$

$$\bar{v}_{\alpha} = v_{\alpha 0} + \bar{v}_{\alpha}'$$

$$P_{\alpha} = P_{\alpha 0} + P_{\alpha}'$$

(3.4)

$$\bar{E} = \bar{E}_0 + \bar{E}'$$

$$\bar{B} = \bar{B}_0 + \bar{B}'$$

where the first quantity on the right hand side is the unperturbed ionospheric parameter, and the second is the perturbation due to the passage of the wave. To simplify matters,  $v_{\alpha 0}$  and  $\bar{E}_0$  might be taken to be negligible. The perturbed counterparts of Equations (3.1) and (3.2) would be solved simultaneously for  $\bar{v}_{\alpha}$  in terms of  $\bar{E}$ , which would then be substituted into the equation for the electric polarization to obtain the constitutive relations with the susceptibility matrix, and finally the dielectric tensor. It is not relevant here to study the propagation in this manner, however, since the total effect of the ionosphere on the received wave is what is desired. Not only will  $v_{\alpha 0}$  and  $\bar{E}_0$  be neglected, but  $N_{\alpha}'$  as well. Then if non-linear terms in the perturbed quantities, the  $\alpha$ th constituent's velocity and the wave-fields, are neglected, the terms

$$m_{\alpha} (\bar{v}_{\alpha} \cdot \bar{\nabla}) \bar{v}_{\alpha}$$

$$z_{\alpha} e \bar{v}_{\alpha} \times \bar{B}_{\text{wave}}$$

are dropped. This eliminates the need for Equation (3.1). The Lorentz polarization term has been excluded, on the basis of experimental evidence discussed by Budden (1961).

If only a one component plasma is considered, that is, if only the motion of the electrons is considered and not the motion of the heavier, more sluggish ions, as is proper to do if the number density of ions is not much greater than the number density of electrons, then the summation over  $\alpha$  charged constituents is no longer necessary, and  $z_{\alpha}$  becomes equal to unity. The ions simply cannot respond to the passing wave-fields as rapidly as the electrons, and the motion that they do acquire is too small to be greatly affected by the earth's magnetic field for VLF frequencies, as mentioned by Budden (1961).

Finally, neglecting the effects of gravity and the thermal pressure gradient (3.2) reduces to

$$e\bar{E}_{\text{wave}} + e\frac{\partial\bar{r}}{\partial t} \times \bar{B}_{\text{earth}} = m\frac{\partial^2\bar{r}}{\partial t^2} + m\nu\frac{\partial\bar{r}}{\partial t}, \quad (3.5)$$

where the ionospheric electric fields have also been neglected. The collision frequency,  $\nu$ , is now that for electrons with ions, electrons, and neutrals, but since the number density of neutrals is so much greater than that of ions, and electrons it may be effectively taken as the collision frequency for electron-neutral collisions. This collision frequency, however, is dependent upon the energy of the electrons, this fact being taken into account by Sen and Wyller (1960) in a generalization of Appleton-Hartree magnetoionic theory.

The inclusion of this energy dependence makes Equation (3.5) invalid, but it can still be used to give good results for VLF studies if the correct collision frequency profile is used, as shown by Deeks (1966a). The use of such an effective collision frequency profile is a mathematical device to equate, as far as possible, the two theories. The profiles of collision frequency for monoenergetic electrons of energy  $kT$  used in Sen-Wyller theory and for the effective collision frequency used to make Appleton-Hartree theory give fairly good agreement with the Sen-Wyller results for VLF calculations are shown in Figure 3.1. The dashed curve should be used for all calculations employing the theory of this chapter. The penalty for doing so, according to Deeks (1966a) is slightly increased absorption (smaller reflection coefficient magnitudes) relative to results obtained by using Sen-Wyller theory, but the difference between the results is less than experimental error, especially at VLF frequencies.

Although the wave at the transmitter is spherical, far from the antenna in a localized region it can be approximated by a plane wave of the form

$$e^{i\omega t - ik\bar{r}}$$

Thus  $\frac{\partial}{\partial t}$  in (3.5) can be replaced by  $i\omega$  to produce an equation in the transform domain. Multiplying this transformed version of (3.5) by  $Ne/m\omega^2$ , where  $\omega$  is the angular wave-frequency, and noting that the electric polarization,  $\bar{P}$ , and geomagnetic field vector,  $\bar{Y}$ , are given by

$$\bar{P} = Ne\bar{r} \quad (3.6)$$

$$\bar{Y} = \frac{e}{m\omega} \bar{B} \quad (3.7)$$

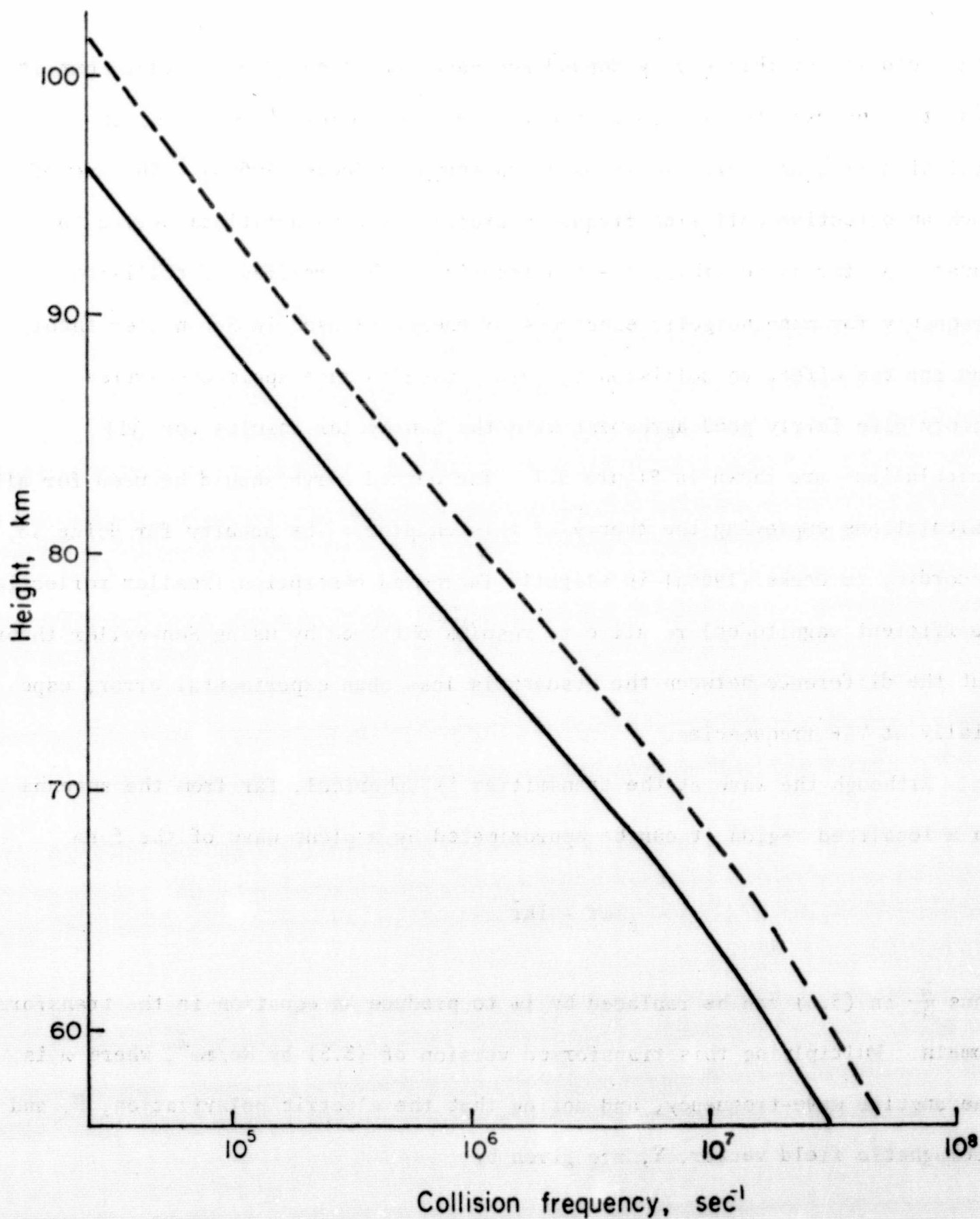


Figure 3.1 Height variation of  $\nu_M$ , the collision frequency of mono-energetic electrons of energy  $kT$  (full curve) and  $\nu_{eff}$ , the effective classical collision frequency for very long wave calculations (dashed curve), (after Deeks, 1966a).

it is a straightforward matter to obtain the constitutive relations for the ionosphere. These are of the matrix form

$$\bar{P} = \epsilon_0 \hat{M} \bar{E} \quad (3.8)$$

where  $\hat{M}$  is the susceptibility tensor given by

$$\hat{M} = \frac{-X}{U(U^2 - Y^2)} \begin{pmatrix} U^2 - l^2 Y^2 & -iUnY - lmY^2 & iUmY - lnY^2 \\ iUnY - lmY^2 & U^2 - m^2 Y^2 & -iUlY - mnY^2 \\ -iUmY - lnY^2 & iUlY - mnY^2 & U^2 - n^2 Y^2 \end{pmatrix} \quad (3.9)$$

The quantities of which the susceptibility matrix is composed are

$$X = \frac{Ne^2}{\epsilon_0 m \omega^2} = \frac{\omega_p^2}{\omega^2} \quad (3.10)$$

$$Y = |\bar{Y}| = \left| \frac{e\bar{B}}{m\omega} \right| = \frac{\omega_H}{\omega} \quad (3.11)$$

$$U = 1 - iZ = 1 - i \frac{v}{\omega} \quad (3.12)$$

where  $\omega_H$  is the gyrofrequency for electrons or the cyclotron frequency, and  $\omega_p$  is the plasma frequency at the altitude corresponding to  $N(z)$ . The letters  $l, m, n$  represent the direction cosines of the geomagnetic field vector,  $\bar{Y}$ , with respect to a right-handed coordinate system whose  $z$  axis is vertically upward and whose positive  $x$  axis is in the direction of the horizontal component of the wave vector,  $\bar{k}$ . The direction cosines are given by



$$\begin{aligned}
 l &= -\cos \phi \cos \alpha \\
 m &= -\cos \phi \sin \alpha \\
 n &= \sin \phi
 \end{aligned}
 \tag{3.13}$$

where  $\phi$  is the magnetic dip angle, measured down from the horizontal ( $0 < \phi \leq 90^\circ$  for Northern Hemisphere), and  $\alpha$  is the azimuth east of magnetic north of the x axis, which is in the plane of propagation. The coordinate system is shown in Figure 3.2.

A point which often generates much confusion is that Y can be defined so that the gyrofrequency for electrons is negative

$$Y = \frac{e|\bar{B}|}{m\omega}
 \tag{3.14}$$

If this is done, however, the signs of the direction cosines are changed, which means that they are the direction cosines of  $\bar{B}$ , which is oppositely directed to  $\bar{Y}$ . The use of either set of definitions for Y, l, m, and n will yield the same susceptibility matrix elements.

One other point worthy of mention is that the expression for  $\bar{P}$  used in Equation (3.6) is the result of taking an average over a volume containing many electrons. The polarization vector and the wave fields used later in Maxwell's equations are assumed fairly constant over distances much less than a wavelength, but large compared with inter-electron distances even for a non-slowly varying medium. That is, changes in the electron density in the vertical direction are not neglected, but small irregularities are smoothed out. As Budden (1961) mentions, there would be no meaning in speaking of the value of  $\bar{P}$  at a specific point in the free space between electrons.

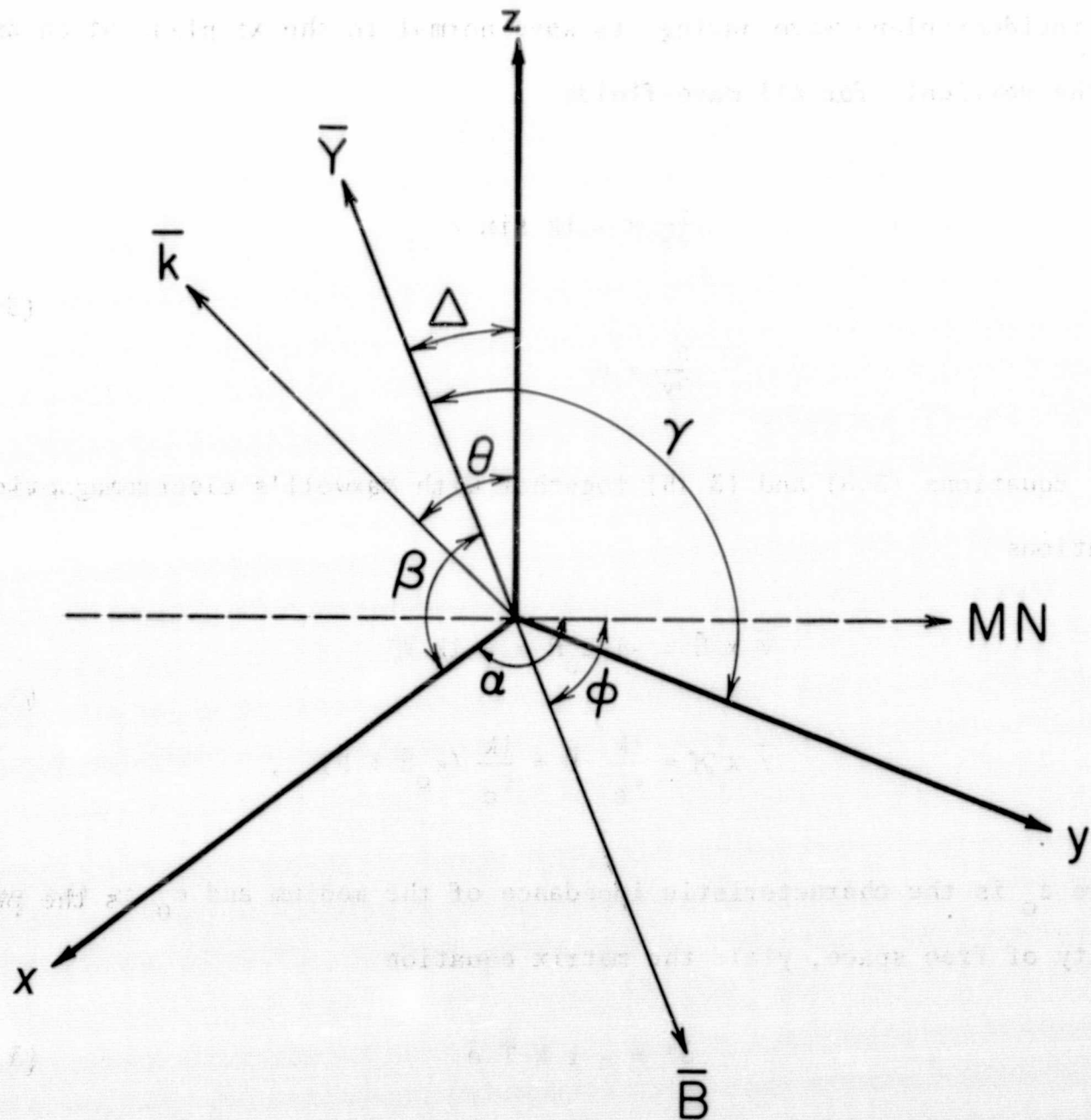


Figure 3.2 The relevant coordinate system at the transmitter. The wave vector  $\vec{k}$  is in the xz plane.  $\vec{B}$  is in the plane of the magnetic meridian.  $\beta$ ,  $\gamma$ ,  $\Delta$  are the arccosines of the direction cosines,  $l$ ,  $m$ ,  $n$  of the geomagnetic field vector,  $\vec{Y}$ .

### 3.2 The Relevant Equations

With the form of the plane wave already assumed below the ionosphere and the incident plane wave having its wave normal in the  $xz$  plane at an angle  $\theta$  to the vertical, for all wave-fields

$$\frac{\partial}{\partial x} = -ik \sin \theta \quad (3.15)$$

$$\frac{\partial}{\partial y} = 0$$

Equations (3.8) and (3.15) together with Maxwell's electromagnetic equations

$$\bar{\nabla} \times \bar{E} = -ikZ_0 \bar{H} = -ik \mathcal{H} \quad (3.16)$$

$$\bar{\nabla} \times \mathcal{H} = \frac{ik}{\epsilon_0} \bar{D} = \frac{ik}{\epsilon_0} (\epsilon_0 \bar{E} + \bar{P}) ,$$

where  $z_0$  is the characteristic impedance of the medium and  $\epsilon_0$  is the permittivity of free space, yield the matrix equation

$$\bar{e}' = -ik \hat{T} \bar{e} \quad (3.17)$$

where the prime is the partial derivative with respect to altitude, and

$$\bar{e} = \begin{pmatrix} E_x \\ -E_y \\ \mathcal{H}_x \\ \mathcal{H}_y \end{pmatrix} \quad (3.18)$$

and

$$\mathbb{T} = \begin{pmatrix} -\frac{SM_{31}}{1+M_{33}} & \frac{SM_{32}}{1+M_{33}} & 0 & \frac{C^2+M_{33}}{1+M_{33}} \\ 0 & 0 & 1 & 0 \\ \frac{M_{23}M_{31}}{1+M_{33}} - M_{21} & C^2+M_{22} - \frac{M_{23}M_{32}}{1+M_{33}} & 0 & \frac{SM_{23}}{1+M_{33}} \\ 1 + M_{11} - \frac{M_{13}M_{31}}{1+M_{33}} & \frac{M_{32}M_{13}}{1+M_{33}} - M_{12} & 0 & \frac{-SM_{13}}{1+M_{33}} \end{pmatrix} \quad (3.19)$$

where  $S = \sin \theta$ ,  $C = \cos \theta$ , and the  $M_{ij}$  are elements of the susceptibility matrix.  $X$  and  $Z$  are functions of height, since they depend upon the electron density and collision frequency respectively. Therefore the  $M_{ij}$  are functions of height, making the  $T_{ij}$  functions of height. The wave-fields and their derivatives with respect to  $z$  are also naturally functions of height. If it was desired to solve for the actual wave-fields, Equation (3.17) would be treated. Of interest here, however, are the reflection coefficients, which are ratios of the fields at any altitude desired to the incident fields. The reflection coefficient matrix is defined as

$$\mathbb{R} = \begin{pmatrix} R_{||} & R_{\perp} \\ R_{\perp} & R_{||} \end{pmatrix} = \begin{pmatrix} \frac{E_{||}^{(R)}}{E_{||}^{(I)}} & \frac{E_{\perp}^{(R)}}{E_{||}^{(I)}} \\ \frac{E_{||}^{(R)}}{E_{\perp}^{(I)}} & \frac{E_{\perp}^{(R)}}{E_{\perp}^{(I)}} \end{pmatrix} \quad (13.20)$$

where  $E_{||}^{(I)}$  and  $E_{\perp}^{(I)}$  are the components of the incident electric field parallel and perpendicular to the plane of propagation respectively, and  $E_{||}^{(R)}$  and  $E_{\perp}^{(R)}$

are defined similarly for the reflected wave. The dependent variable is then the reflection coefficient matrix and not the wave-field vector. This is the dependent variable used by Budden (1955a). Barron and Budden (1959) resort to another dependent variable, however, termed the admittance matrix  $\tilde{\tilde{A}}$ . It is related to  $\tilde{\tilde{R}}$  by

$$\tilde{\tilde{A}} = \begin{pmatrix} - \left( \frac{(\frac{1}{2}R_{\perp\perp} + 1)}{2RPOLY} + 1 \right) / C & \frac{-1}{2RPOLY} R_{\perp\perp} \\ - \frac{1}{2RPOLY} R_{\parallel\parallel} & - \left( \frac{(\frac{1}{2}R_{\parallel\parallel} - 1)}{2RPOLY} - 1 \right) C \end{pmatrix} \quad (13.21)$$

where

$$RPOLY = \left( \frac{1}{2}R_{\parallel\parallel} - 1 \right) \left( \frac{1}{2}R_{\perp\perp} + 1 \right) - \left( \frac{1}{2}R_{\perp\perp} \right) \left( \frac{1}{2}R_{\parallel\parallel} \right) \quad (13.22)$$

The differential Equations (3.17) become, after this change of variable, in matrix form

$$i\tilde{\tilde{A}} = k \left( \tilde{\tilde{A}} \begin{pmatrix} -T_{11} & T_{12} \\ 0 & 0 \end{pmatrix} + \begin{pmatrix} T_{44} & 0 \\ T_{34} & 0 \end{pmatrix} \tilde{\tilde{A}} + \tilde{\tilde{A}} \begin{pmatrix} -T_{14} & 0 \\ 0 & 1 \end{pmatrix} \tilde{\tilde{A}} + \begin{pmatrix} T_{41} & -T_{42} \\ T_{31} & -T_{32} \end{pmatrix} \right) \quad (13.23)$$

where this correct version is given by Barron and Budden (1959), the version in Budden (1961) being incorrect. This equation is clearly too complicated to be solved analytically. After numerically integrating it down through the ionosphere from a known starting solution, however,  $\tilde{\tilde{R}}$  can be obtained from  $\tilde{\tilde{A}}$  by

$$R_{22} = 2 \begin{pmatrix} -CA_{11} - 1 & A_{12} \\ A_{21} & 1 - A_{22}/C \end{pmatrix}^{-1} + \begin{pmatrix} 1 & 0 \\ 0 & -1 \end{pmatrix} \quad (13.24)$$

The wave admittance approach is used here, although the wave-fields as variables are preferred by others such as Pitteway (1965), and the reflection coefficients as variables by still others such as Sheddy (1968).

## 4. FULL-WAVE SOLUTIONS

### 4.1 The Starting Solution

The starting solution necessary to initiate the solution of the relevant differential equations from the full-wave theory of Chapter 3 can be obtained by the method of Sheddy (1968). This method does not depend on a lengthy, and often too slowly converging, preliminary integration, beginning with a crude estimate of the initial solution, down through a fictitious homogeneous ionosphere with  $X$  and  $Z$  held constant at their values at the height where the preliminary integration is started. This was the method of Budden (1955a). Such a preliminary integration is terminated when  $\tilde{A}'$  is arbitrarily close to zero, and the resultant  $\tilde{A}$  is the admittance matrix corresponding to only up-going waves above the boundary, that is, the matrix for a sharply bounded homogeneous medium. This result may then be used as the starting solution back at the starting level for the preliminary integration, since once  $\tilde{A}$  is found which satisfies  $\tilde{A} = 0$ , it will not change over a homogeneous ionosphere. Clearly, this starting level must be well above the height in the real ionosphere where waves of a given frequency are interacting with the ionization. The same method could be used if  $\tilde{R}$  were the dependent variable, but the rate of convergence to  $\tilde{R}' = 0$  would be different.

That the problem is reduced to one of a sharp boundary makes appropriate the boundary matching technique of Crombie (1961), which in turn employs the solutions to the Booker quartic equation with complex coefficients discussed in Chapter 2. The Booker quartic roots may be obtained in closed form using the mathematics of Burnside and Panton (1904). Whereas Crombie's solution was good only for west-east or east-west propagation, Sheddy's method gives

the reflection coefficients for a plane of propagation of arbitrary azimuth east of north for a sharply bounded homogeneous ionosphere with a lower boundary at the height where one wishes to commence a full-wave solution.

The flow chart for the initial solution portion of the full-wave program is shown in Figure 4.2, the actual computer printout being given in the Appendix. Flow chart notation follows that of McCracken (1965). This flow chart is preceded by the flow chart in Figure 4.1 for the input portion of the main program, in which all quantities necessary for later calculations are defined or computed.

#### 4.2 The Numerical Integration

Once the initial solution has been found, the numerical integration down through the real ionosphere is carried out using a modified Runge-Kutta process due to Gill (1951). The pertinent constants of nature, input parameters (indicated by asterisks) and integration variables are defined below. The left-hand symbol is the standard notation; the right-hand symbol is the notation used in the computer program, if it differs from the standard notation. MKS units are used in all calculations. All calculations are performed with double precision accuracy.

e	Charge of the electron (it is negative).
m,ELECM	Mass of the electron.
$\epsilon_0$ ,PERME	Permittivity of free space.
$\mu_0$ ,PERMM	Permeability of free space.
c	Speed of light in a vacuum.
B	Magnitude of earth's magnetic field.
$\theta$ ,THETA(in radians)	Angle of incidence between the vertical and the wave normal of the incident wave below the ionosphere.
* ANGLE(in degrees)	



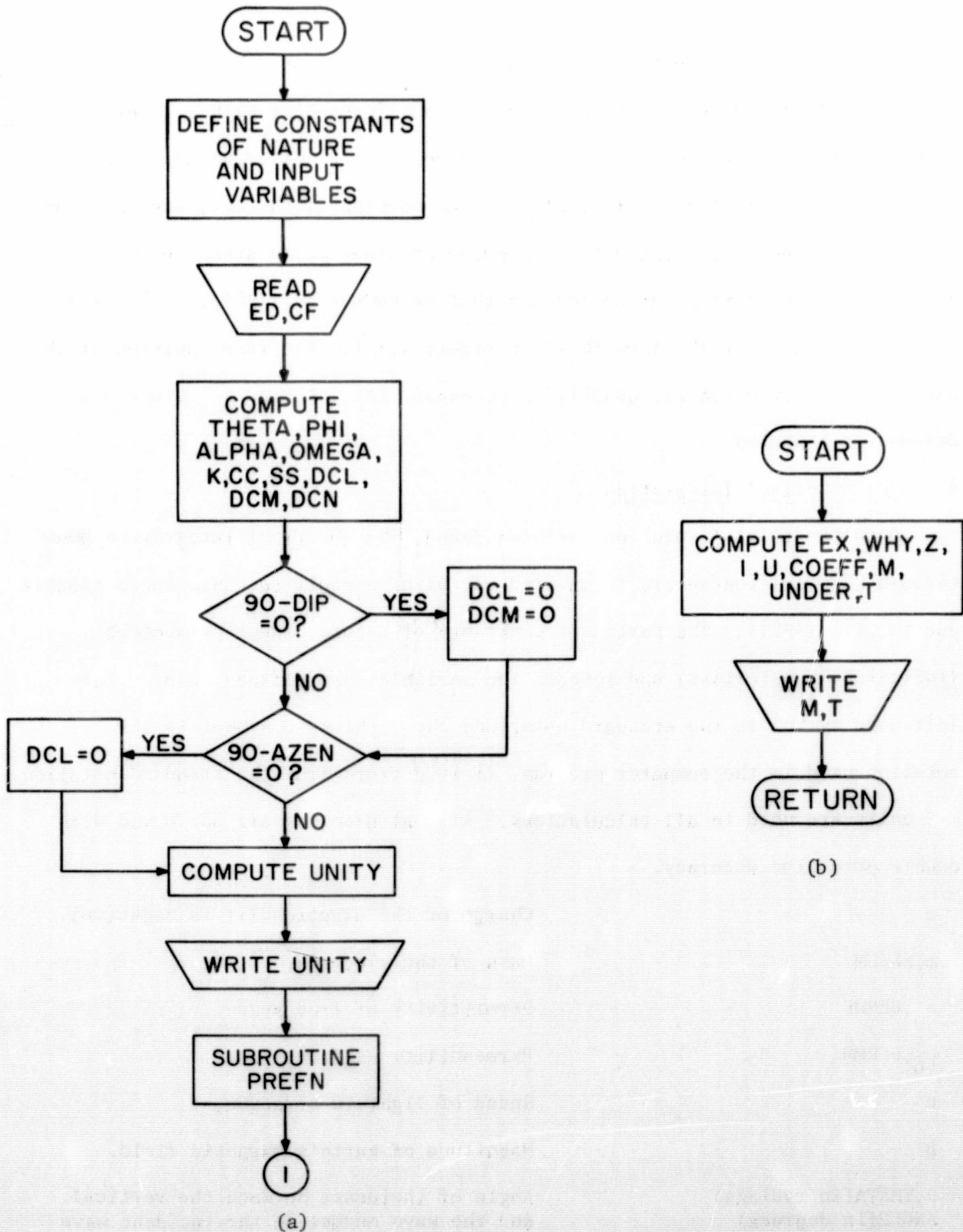


Figure 4.1 Flow chart depicting (a) input portion of main program, including (b) subroutine PREFN.

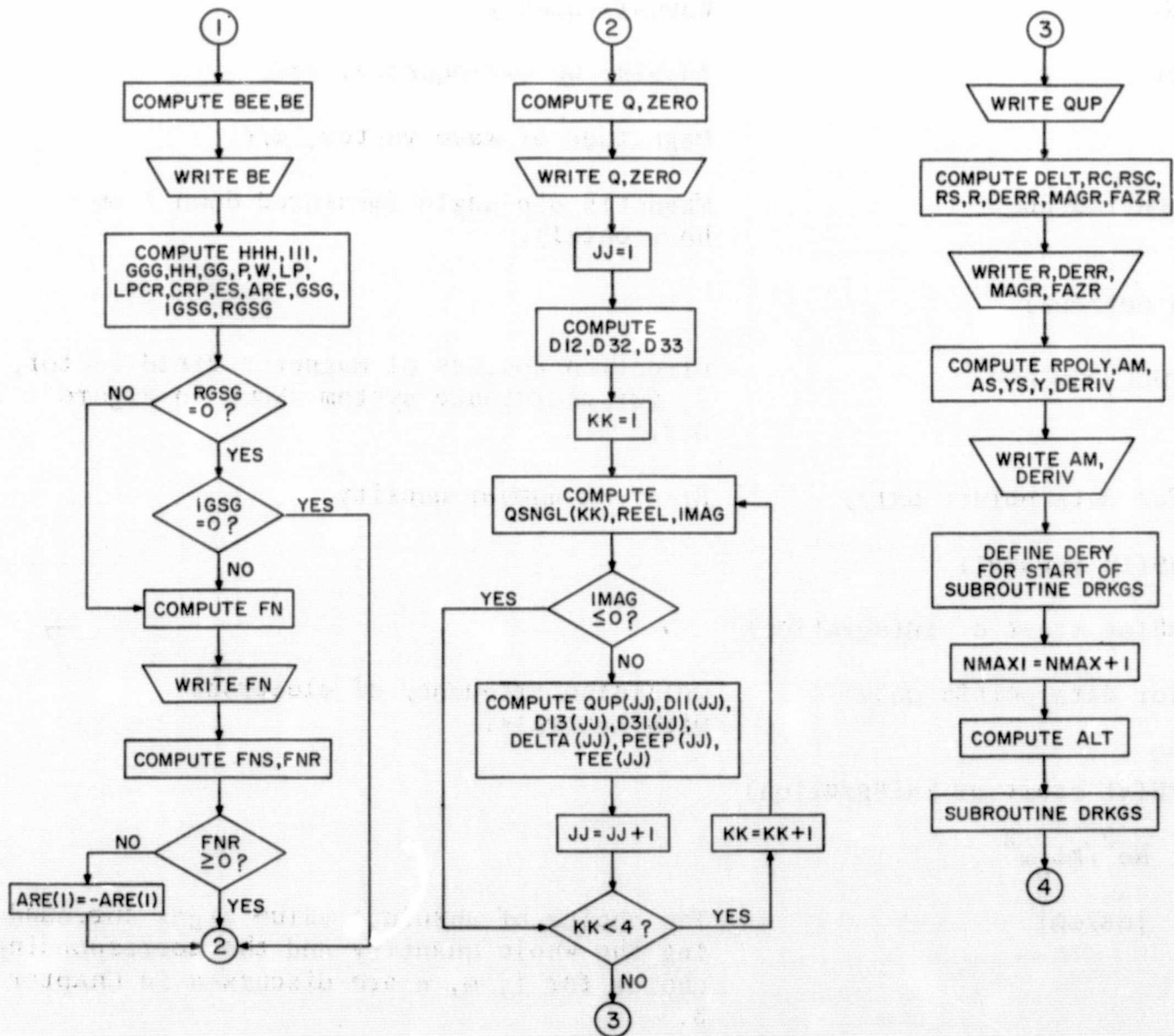


Figure 4.2 Flow chart depicting initial solution (after Sheddy, 1968) portion of main program.

$\alpha$ ,ALPHA(in radians)	Azimuth east of magnetic north of positive x axis in the plane of propagation.
* AZEN(in degrees)	
* f, FREQ	Wave-frequency.
$\omega$ ,OMEGA	Angular wave-frequency, $2\pi f$ .
k	Magnitude of wave vector, $\omega/c$ .
$\phi$ ,PHI(in radians)	Magnetic dip angle (measured down from horizontal).
* DIP(in degrees)	
l,m,n;DCL,DCM,DCN	Direction cosines of magnetic field vector, $\bar{Y}$ , for coordinate system shown in Figure 3.2.
* N,ED(For data points only)	Electron number density.
EDENS(in general)	
EDPRE(at start of integration)	
* $\nu$ ,CF(for data points only)	Collision frequency of electrons with neutrals.
CFREQ	
CFPRE(at start of integration)	
X,EX $N_e^2/m\epsilon_0\omega^2$	
Y,WHY $ eB/\omega m $	The choice of absolute value signs surrounding the whole quantity and the corresponding choice for l, m, n are discussed in Chapter 3.
Z	$\nu/\omega$
i	$\sqrt{-1}$
$\hat{M}$ ,M=MR+iMI	Susceptibility matrix.
$\hat{T}$ ,T=TR+iTI	T matrix.
q	Root of Booker quartic equation.
$R_{11} = \begin{vmatrix} R_{11} \\ R_{12} \\ R_{21} \\ R_{22} \end{vmatrix}$ ,RC(1)=R(1)+iR(5)	Elements of reflection coefficient matrix, R

$R_{12} = \frac{R_1}{R_2}, RC(2) - R(2) + iR(6)$   
 $R_{21} = \frac{R_1}{R_2}, RC(3) = R(3) + iR(7)$   
 $R_{22} = \frac{R_1}{R_2}, RC(4) = R(4) + iR(8)$   
 $\tilde{R}$ , MAGR Matrix of reflection coefficient magnitudes or amplitudes  
 $\tilde{R}$ , FAZR Matrix of reflection coefficient phases or arguments  
 $\tilde{R}'$ , DERR Matrix of reflection coefficient derivatives with respect to altitude  
 $A_{11}, AM(1) = Y(1) + iY(5)$  Elements of wave admittance matrix,  $\tilde{A}$   
 $A_{12}, AM(2) = Y(2) + iY(6)$   
 $A_{21}, AM(3) = Y(3) + iY(7)$   
 $A_{22}, AM(4) = Y(4) + iY(8)$   
 $\tilde{A}'$ , DERIV Matrix of wave admittance derivatives with respect to altitude  
 $DERIV(I) = DERY(I) + iDERY(I+4)$   
\* NMAX The number of data points comprising the digitized form of the electron density profile (same for collision frequency profile).  
\* PRMT(1) Height at start of integration.  
\* PRMT(2) Height at end of integration.  
\* PRMT(3) Integration interval.  
\* PRMT(4) Accuracy maintained per step in the integration.  
\* ZDATA Height interval between data points.  
ALT Altitudes corresponding to data points representing profiles of N and  $\nu$ .  
IHLF Number of times integration interval is halved in order to ensure accuracy supplied in PRMT(4).  
C, CC  $\cos \theta$   
S, SS  $\sin \theta$

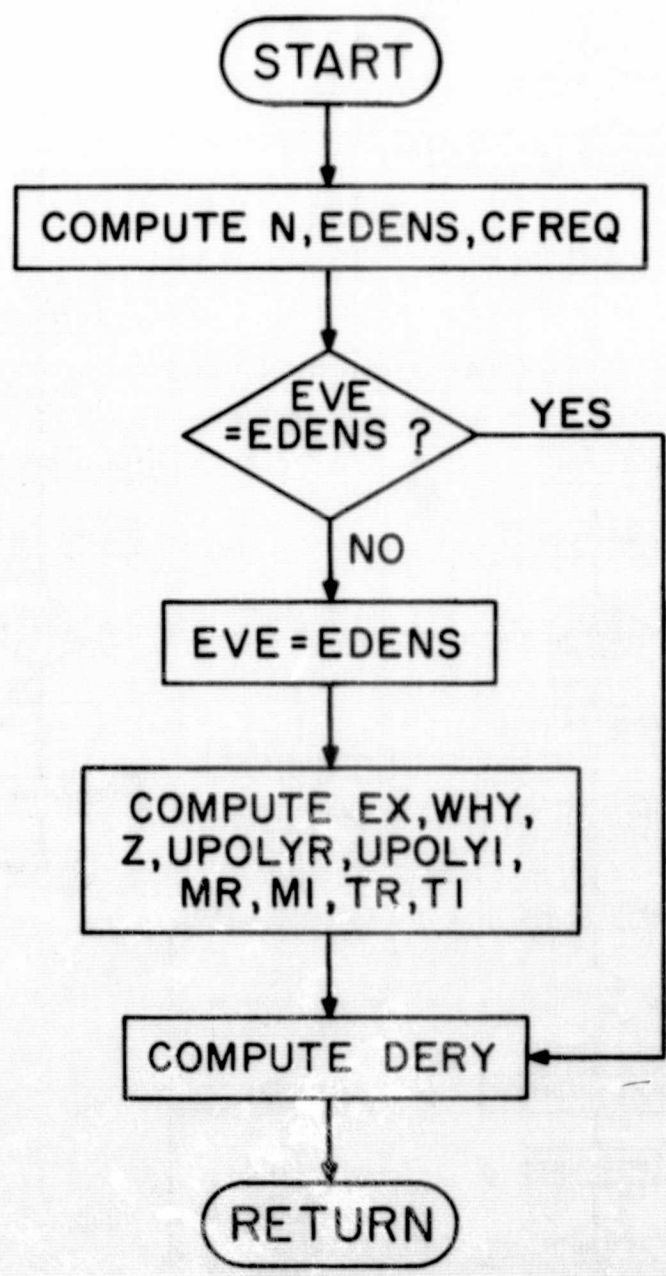
The electron density and collision frequency profiles are specified by data points given every (-ZDATA) meters between PRMT(1) and (PRMT(2) + ZDATA) inclusive. If PRMT(3) < ZDATA, the values in between data points are computed by linear interpolation; no sophisticated fitting of polynomial curves to points is used. PRMT(1) is chosen so that  $EX \approx 100(1+WHY)$  and PRMT(2) so that  $EX < 1$  for the frequency being used. Although these limits are vestiges of ray theory, and should not be considered to be related to precise levels of reflection for VLF waves, they give reasonable boundaries for the region of significant wave-ionosphere interactions.

The angle of incidence is computed by geometry, knowing the distance between the transmitter and receiver, and assuming an average height of reflection equal to the altitude where  $EX = (1+WHY)$ . This height decreases during the sunrise period, causing  $\theta$  to increase.

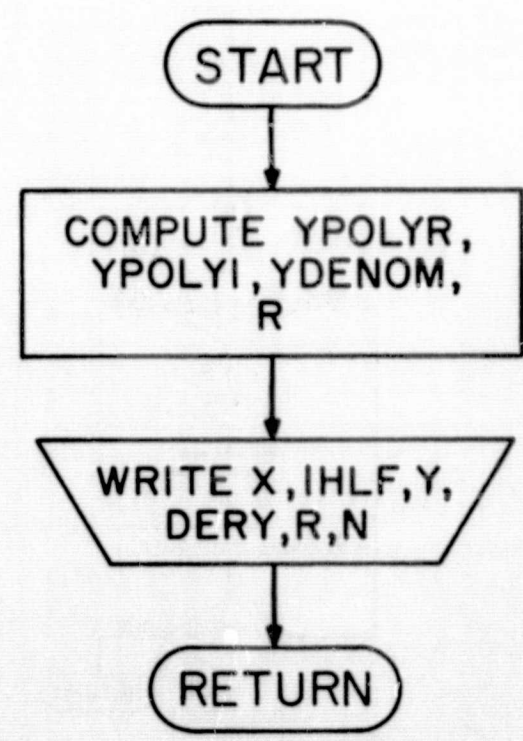
PRMT(3) is chosen small enough so that IHLF does not become too large, yet large enough so that an unnecessary number of calculations over gradual electron density gradients are avoided. PRMT(4) is chosen large enough so that IHLF does not become too large over steep electron density gradients, yet small enough so that the final results are meaningful.

Figure 4.3 shows the flow chart for the DRKGS IBM SSP Library subroutine used in the numerical integration. Figure 4.4 shows the flow chart for the subroutines FCT and OUTF called from within DRKGS. Use of the OUTF subroutine can provide a continuous print-out of the reflection coefficients down through the entire ionosphere, producing diagrams analogous to those of Pitteway (1964), who used the penetrating and non-penetrating wave-fields as dependent variables. The locations for this use of the OUTF subroutine are shown as dashed boxes in Figure 4.3. If this is not desired, the OUTF subroutine is not necessary. The





(a)



(b)

Figure 4.4 Flow chart depicting subroutines (a) FCT and (b) OUTP called from within DRKGS subroutine.

FCT subroutine computes the derivatives of the wave admittances as they steadily change down through the ionosphere because of the changing electron density and collision frequency. Figure 4.5 shows the output portion of the program, which gives the final reflection coefficient values below the ionosphere.

No provision was made to prevent numerical swamping, since with the dependent variables being of the same order of magnitude and the computer having great accuracy when operating in the double precision mode it was felt unnecessary.

#### 4.3 Checks of the Full-Wave Program

A complicated computer program such as the one used in full-wave solutions cannot be used with any confidence until after its results have been thoroughly checked against known results.

The correctness of the starting solutions was verified in several ways. First, the Booker quartic roots were substituted into the Booker quartic equation to see if they satisfied it. The value of the Booker quartic equation, which should strictly be zero, was always at least  $10^2$  times smaller than any of the roots themselves, and often  $10^5$  times smaller.

The starting reflection coefficients and admittance matrix elements were checked by substituting them into the differential equations. The values of the derivatives, which again for an exact solution should be zero, were at least  $10^4$  times smaller than any of the matrix elements themselves, and some of the derivatives were as much as  $10^{17}$  times smaller. In other words, with matrix element magnitudes on the order of unity, the derivatives had magnitudes of  $10^{-4}$  and smaller, or as close to the value zero as one might reasonably expect from a digital computer following all the steps of Sheddy's method while carrying 17 digits in its double precision mode of operation.



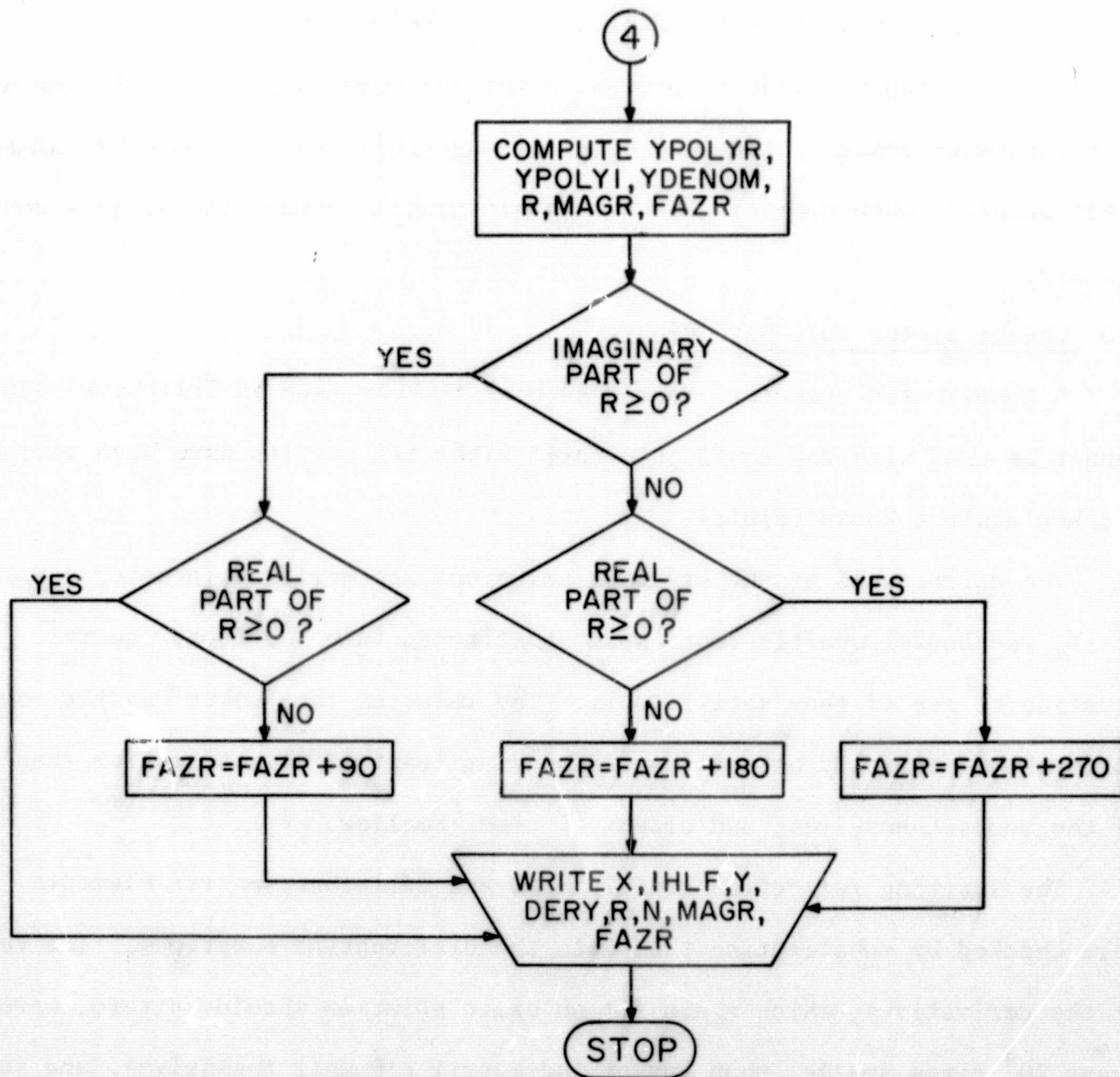


Figure 4.5 Flow chart depicting final output portion of main program.

In addition, a comparison was made with results of initial solutions numerically calculated by Fedor, et al., (1964) for the special case of west-east propagation. Table 4.1 shows the results of the comparison, with all numbers rounded off to 2 places to the right of the decimal for brevity.

The numerical integration and the resulting final solutions were checked by comparing results with those of Budden (1955b), who in turn compared his results with the analytic solutions of Heading and Whipple (1952). The comparison was made for the case of vertical incidence, an exponential electron density profile, a constant collision frequency, a vertically downward magnetic field, and west-east propagation. Figure 4.6a shows Budden's comparison with Heading and Whipple for  $X = \exp(.295z)$  and  $Z = 8$  where  $z$  is in km. Points marked X were calculated by the author. A similar comparison is shown in Figure 4.6b, but the electron density gradient is sharper,  $X = \exp(2.36z)$ , and  $Z = 2$ .

A further comparison was made with the computing facilities at NELC and the Radio Research Station, Slough, England. For this check only, the collision frequency profile of Fejer and Vice (1959) was used, along with the nighttime electron density profile of Deeks (1964). The angle of incidence was taken to be  $40^\circ$ , the dip angle  $70^\circ$ , the azimuth of the propagation path  $152^\circ$ , and the wave-frequency 21.4 KHz. The numerical integration was started at 108.00 km and stopped at 63.55 km. Table 4.2 compares the results.

All of the comparisons made indicate that full-wave calculations with the program described can be used with reasonable confidence to find the variation of the reflection coefficient matrix under different circumstances, even for an ionosphere with steep electron density gradients.

TABLE 4.1

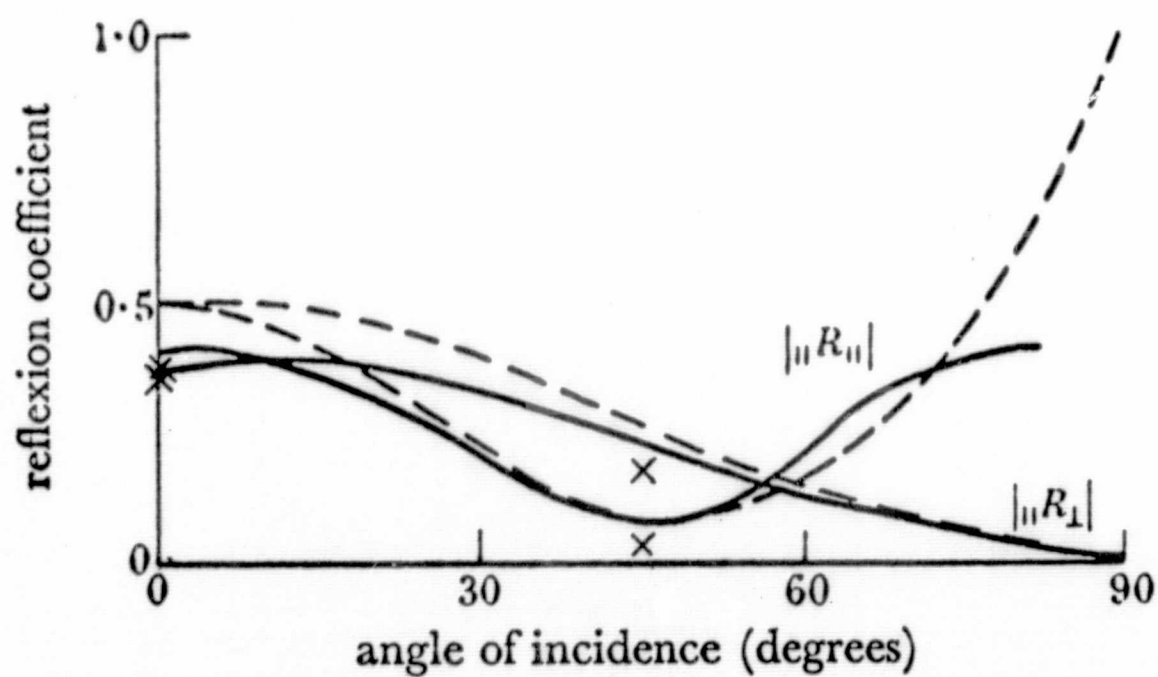
A comparison of the author's numerically calculated Starting solutions with those of Fedor, et al., (1964) of NELC.

	$\begin{matrix} \text{R} \\ \parallel \\ \text{R} \end{matrix}$	$\begin{matrix} \text{R} \\ \parallel \\ \perp \end{matrix}$	$\begin{matrix} \text{R} \\ \perp \\ \parallel \end{matrix}$	$\begin{matrix} \text{R} \\ \perp \\ \perp \end{matrix}$
NELC	$9.66 \times 10^{-1} - i3.43 \times 10^{-2}$	$3.31 \times 10^{-2} + i3.05 \times 10^{-2}$	$3.31 \times 10^{-2} + i3.05 \times 10^{-2}$	$-9.68 \times 10^{-1} + i3.24 \times 10^{-2}$
VIERTEL	$9.48 \times 10^{-1} - i5.28 \times 10^{-2}$	$5.08 \times 10^{-2} + i4.51 \times 10^{-2}$	$5.08 \times 10^{-2} + i4.51 \times 10^{-2}$	$-9.51 \times 10^{-1} + i4.97 \times 10^{-2}$
	$A_{11}$	$A_{12}$	$A_{21}$	$A_{22}$
NELC	15.26-i15.11	14.96-i15.25	14.96-i15.25	-15.39+i15.11
VIERTEL	9.91-i 9.82	9.75-i 9.97	9.74-i 9.97	-10.05+i 9.81
	$A'_{11}$	$A'_{12}$	$A'_{21}$	$A'_{22}$
NELC	$-1.48 \times 10^{-5} - i3.01 \times 10^{-4}$	$3.02 \times 10^{-4} + i1.48 \times 10^{-5}$	$3.02 \times 10^{-4} + i1.48 \times 10^{-5}$	$1.49 \times 10^{-5} + i3.03 \times 10^{-4}$
VIERTEL	0.00 $-i3.20 \times 10^{-17}$	$6.97 \times 10^{-6} - i8.19 \times 10^{-6}$	$-2.28 \times 10^{-17} + i2.74 \times 10^{-17}$	$-5.97 \times 10^{-8} - i3.52 \times 10^{-9}$

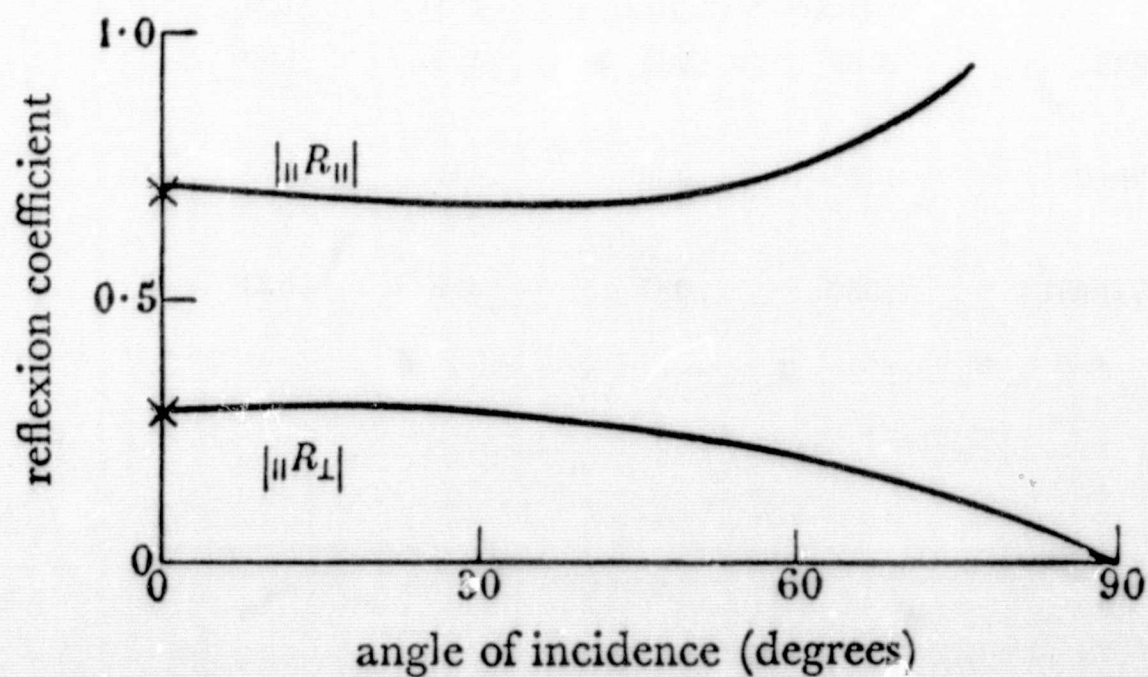
TABLE 4.2

A comparison of full-wave solutions for the nighttime electron density profile of Deeks (1964) and the collision frequency profile of Fejer and Vice (1959).

	$ R_{  } $	$ R_{\perp} $	$ R_{  } $	$ R_{\perp} $
RRS	.088	.089	.408	.509
NELC	.085	.088	.436	.573
VIERTEL	.057	.087	.458	.621



(a)



(b)

Figure 4.6 A comparison of the full-wave results, reflection coefficient magnitude vs angle of incidence, for  $\nu$  constant,  $\phi = 90^\circ$ , and  $\alpha = 90^\circ$ , of (a) Budden (1955b) (solid line), Budden using the formulas of Heading and Whipple (1952) (dashed line), and the author (points marked x) for  $X = \exp(.295z)$ ,  $Z = 8$  and (b) Budden (1955b) (solid line) and the author (points marked x) for  $X = \exp(2.36z)$ ,  $Z = 2$ .

#### 4.4 Suggestions for Applications of the Full-Wave Program

One important application of the full-wave program would be to test the consistency of theoretical and experimental methods of studying the D region by comparing the temporal behavior of the reflection coefficient matrix over the sunrise period obtained by full-wave solutions with the results from ground-based VLF studies. For the electron density profiles used in the full-wave program, the results of Smith et al. (1966), shown in Figure 4.7, might be used, with suitable lower E region profiles added to the upper portions of the curves to extend them to sufficiently high levels where the integration would be started. For experimental VLF results, those given by Sechrist (1968) might be employed. The results of both Smith and Sechrist were obtained during a period of minimum solar activity, but their measurements were made at mid-latitudes in different hemispheres. Also, Smith's profiles were not all determined in the same season. Clearly, the optimum comparison would involve data obtained at the same place and time, but such information is regrettably scarce.

Another valuable comparison would involve replacing Smith's electron density profiles above, which were deduced from ground-based experiments, with profiles obtained from rocket measurements, such as those of Mechtly and Smith (1968) shown in Figure 4.8. The degree of agreement of the theoretical results, obtained using both sets of sunrise electron density profiles, with the experimental VLF results might solve the controversy over which measurement technique is better for measuring electron densities.

If the degree of agreement between theory and experiment proved to be good, more confidence could be displayed in studying not only the sunrise period, but the similar sunset and eclipse conditions by the theoretical and

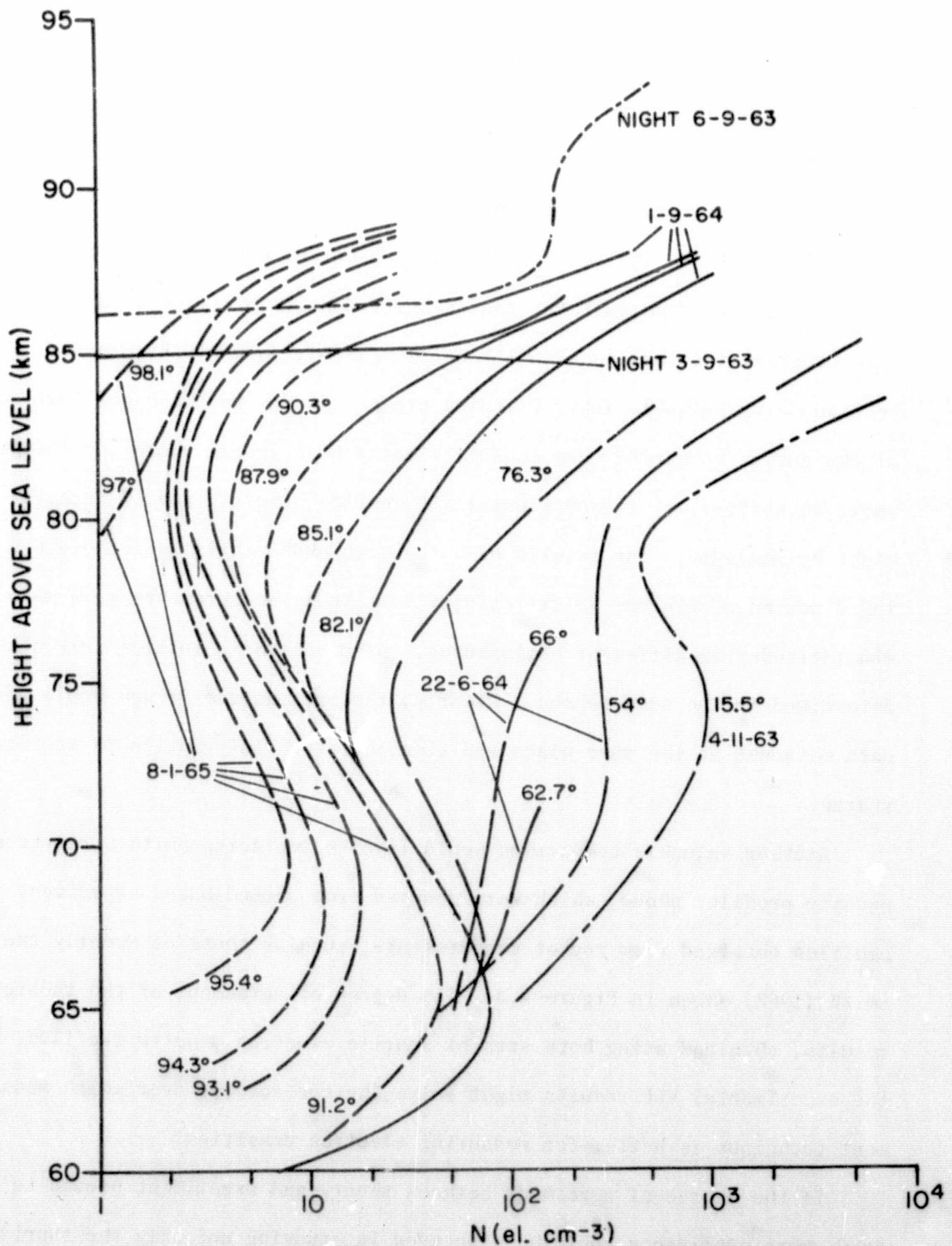


Figure 4.7 D-region electron density profiles for night, dawn, and daytime periods (after Smith *et al.*, 1966) deduced from ground-based measurements.

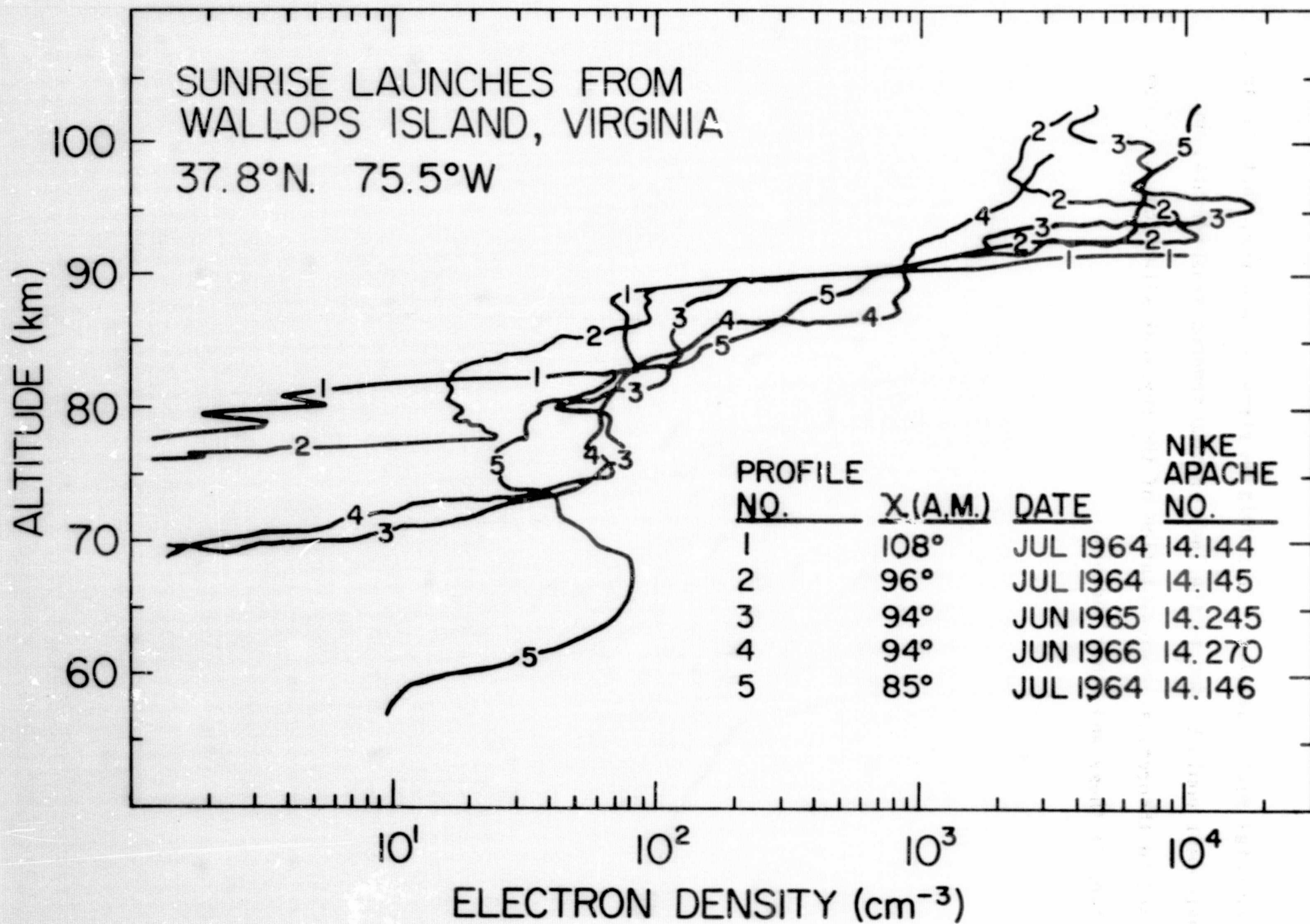


Figure 4.8 D-region electron density profiles over the sunrise period measured with rockets (after Mechtly and Smith, 1968).



experimental means now used. It should be stressed, however, that the lack of agreement could be due to the lack of simultaneous measurements, an incomplete theoretical representation of the physical situation, or a combination of these and other factors.

APPENDIX

The full-wave computer program printout is shown for a sample application, that of finding the reflection coefficients for a sunrise electron density profile. The flow charts for this program are given in Figures 4.1-4.5.

```

$JOB          KP=29,LINES=3000,TIME=900,PAGES=100
1  DIMENSION PRMT(5),DERY(8),AUX(8,8),ED(119),CF(119),ALT(120), VARIABLE
   CTR(4,4),TI(4,4),MR(3,3),MI(3,3),Y(8),R(8),MAGR(4),FAZR(4),T(4,4),
   CDERIV(4), QSNGL(4),RSC(4), M(3,3),BEE(5),BE(4),W(3),ES(3),ARE(3),
   CQ(4),QUP(2),D11(2),D13(2),D31(2),DELTA(2),PEEP(2),TEE(2),RC(4),
   CAM(4),ZERO(4),AMS(4),RS(8),YS(8),DERR(4)
2  REAL*4 FNR,SNGL,REAL,AIMAG,REEL,IMAG,RGSG,IGSG,RS,YS
3  REAL*8 PRMT,Y,DERY,PERME,PERMM,E,EX,WHY,Z,C,B,OMEGA,K,FREQ,DCL,
   CDCM,DCN,ELECM,PHI, THETA,CC,SS,X,ED,CF,PI,UNITY,MAGR,FAZR,R,
   CDCOS,DSIN,DABS,TR,TI,MR,MI,UR,UI,EDPRE,CFPRE,ALPHA, AUX,UPOLYR,
   CUPOLYI,YPOLYR,YPOLYI,UDENOM,DSQRT, DBLE,ALT, DATAN,MDENOM,YDENOM
   C,ANGLE,DIP,AZEN,ZDATA
4  COMPLEX*8 CSQRT,CMLPX,CLOG,CEXP,GSG,FNS,QSNGL,RSC,AMS
5  COMPLEX*16 M,HH,GG,BEE,BE,HHH,III,GGG,ARE,Q,QUP,ZERO,D11,D12,
   CD13,D31,D32,D33,DELTA,PEEP,TEE,DELT,RC,AM,RPOLY,P,LP,LPCR,CRP,ES,
   CFN,CDLOG,CDEXP,CDSQRT,DCMLPX,W,DCONJG,U,I,COEFF
   C,T,DERIV,DERR,CYU,ZIP
6  EXTERNAL FCT,OUTP
   C
   C THE FOLLOWING ARE CONSTANTS OF NATURE
   C E IS THE ELECTRON CHARGE
   C ELECM IS THE ELECTRON MASS
   C PERME IS THE ELECTRIC PERMITTIVITY OF FREE SPACE
   C PERMM IS THE MAGNETIC PERMEABILITY OF FREE SPACE
   C C IS THE SPEED OF LIGHT IN A VACUUM
   C B IS THE EARTH'S MAGNETIC FIELD
   C THE FOLLOWING ARE INPUT VARIABLES
   C THETA IS THE ANGLE OF INCIDENCE
   C PHI IS THE MAGNETIC DIP ANGLE, MEASURED FROM THE HORIZONTAL.
   C IF B FIELD DIPS DOWN AS IN NORTHERN HEMISPHERE, PHI IS POSITIVE
   C AND 0<PHI<90. IF B FIELD DIPS UP AS IN SOUTHERN HEMISPHERE,
   C PHI IS NEGATIVE AND -90<PHI<0.
   C ALPHA IS THE AZIMUTH OF PROPAGATION, MEASURED EAST OF MAGNETIC
   C NORTH, THAT IS, IT IS THE ANGLE BETWEEN MAGNETIC NORTH AND THE
   C POSITIVE X AXIS, WHERE THE XZ PLANE IS THE PLANE OF PROPAGATION.
   C POSITIVE Z IS UPWARDS, POSITIVE X IS IN THE DIRECTION OF THE
   C HORIZONTAL COMPONENT OF K, THE WAVEVECTOR. THE COORDINATE
   C SYSTEM IS RIGHT-HANDED.
   C FREQ IS THE FREQUENCY OF THE INCIDENT PLANE WAVE
   C ED IS THE ELECTRON DENSITY, WHICH IS A FUNCTION OF CHI, THE
   C SOLAR ZENITH ANGLE, AS WELL AS ALTITUDE (ED PROFILE IS ONDATA
   C CARDS)
   C CF IS NU, THE COLLISION FREQUENCY(CF PROFILE IS ON DATA CARDS)
   C CF IS THE NUMBER OF COLLISIONS PER SEC EACH ELECTRON MAKES, NOT THE
   C NUMBER OF ELECTRONS COLLIDING PER SEC
   C X = ALTITUDE
   C DCL, DCM, DCN ARE THE DIRECTION COSINES OF-B WITH RESPECT TO
   C A COORDINATE SYSTEM WHOSE XZ PLANE IS THE PLANE OF INCIDENCE AND
   C WHOSE Z AXIS VERTICAL.
   C ALL VALUES ARE IN MKS UNITS
7  E = -1.6021D-19
8  ELECM = 9.1091D-31
9  PERME = 8.8542D-12
10 PERMM = 1.25664D-6
11 C = 2.997925D8
12 PI = 3.141593D0
13 B = 0.56D-4
   C
14 CHI = 95.4
15 ANGLE = 37.8D0
16 DIP = 70.0D0
17 AZEN = 152.0D0
18 FREQ = 21.40D3
19 NMAX = 119
20 EDPRE = 3.70D10
21 CFPRE = 9.40D04
22 PRMT(1) = 94000.0D0
23 PRMT(2) = 64750.0D0
24 PRMT(3) = -25.0D0
25 PRMT(4) = .00100D0
26 ZDATA = -250.0D0
   NDIM = 8

```

```

27 READ(5,25) ED,CF
28 25 FORMAT(11(1P10D8.2/),1P9D8.2/(1P1D8.2))
C THE FOLLOWING VARIABLES ARE FUNCTIONS OF THE ABOVE INPUT VARIABLES
29 THETA =ANGLE*PI/180.000
30 PHI = DIP * PI / 180.000
31 ALPHA = AZEN*PI/180.000
32 OMEGA =2.000* PI * FREQ
33 K = CMEGA / C
34 CC = DCOS(THETA)
35 SS = DSIN(THETA)
36 DCL =-DCOS(PHI) * DCOS(ALPHA)
37 DCM =-DCOS(PHI) * DSIN(ALPHA)
38 DCN =+DSIN(PHI)
C THE FOLLOWING CARDS ENSURE THE CORRECT VALUES OF DCL AND DCM.
C THEY ARE NECESSARY BECAUSE OF THE FINITE ACCURACY OF THE COMPUTER.
39 IF(90.000 - DIP)92,91,92
40 91 DCL = C.000
41 DCM = C.000
42 92 IF(90.000 - AZEN)94,93,94
43 93 DCL = C.000
44 94 UNITY = DCL*DCL + DCM*DCM + DCN*DCN CHECK
45 WRITE(6,1) UNITY CHECK
46 1 FORMAT(25X,5HUNITY/20X,1P1D19.10//) CHECK
C BEGIN CALCULATION OF INITIAL SOLUTIONS USING METHOD OF SHEDDY.
47 CALL PREFN(M,T,SS,CC,DCL,DCM,DCN,EDPRE,CFPRE,OMEGA,ELECM,
C PERME,E,K,B)
48 BEE(4) =1.000+ M(3,3)
49 BEE(3) = SS * (M(1,3) + M(3,1))
50 BEE(2) = -(( CC* CC) + M(3,3)) *(1.000+ M(1,1)) + (M(1,3)*M(3,1))
C+(M(2,3)*M(3,2))- (1.000+ M(3,3)) * (( CC* CC) + M(2,2))
51 BEE(1) = SS*(M(1,2)*M(2,3) + M(2,1)*M(3,2) -(( CC* CC) + M(2,2))
C*(M(1,3) + M(2,1)))
52 BEE(5) =(1.000+ M(1,1))*(( CC* CC) + M(2,2))*(( CC* CC) + M(3,3))
C+M(1,2)*M(2,2)*M(3,1) + M(1,3)*M(2,1)*M(3,2) -M(1,3)*(( CC* CC)+
CM(2,2))*M(3,1)-(1.000+ M(1,1))*M(2,3)*M(3,2) -M(1,2)*M(2,1)*((
C CC* CC) + M(3,3))
53 BE(3) = BEE(3)/(4.000*BEE(4))
54 BE(2) = BEE(2)/(6.000*BEE(4))
55 BE(1) = BEE(1)/(4.000*BEE(4))
56 BE(4) = BEE(5)/BEE(4)
57 WRITE(6,3) BE(3),BE(2),BE(1),BE(4)
58 3 FORMAT(25X,2HBE/4(20X,1P2D19.10//))
59 HHH = BE(2) - (BE(2)*BE(3))
60 III = BE(4) - (4.000* BE(3) * BE(1)) + (3.000* BE(2) * BE(2))
61 GGG = BE(1)-(3.000* BE(3) * BE(2)) + (2.000* BE(3) * BE(3) * BE(3))
62 HH = - III/12.000
63 GG = -(GGG *GGG/4.000)-(HHH * ((HHH*HHH) + (3.000* HH )))
64 P = (-GG +CDSQRT((GG*GG) +(4.000* HH*HH*HH)))/2.000
65 W(1) =(1.000,0.000)
66 W(2) = DCPLX(DCOS(2.000*PI/3.000),DSIN(2.000*PI/3.000))
67 W(3) = DCPLX(DCOS(4.000*PI/3.000),DSIN(4.000*PI/3.000))
68 LP =CDLOG(P)
69 LPCR = LP/3.000
70 CRP =CDEXP(LPCR)
71 DO 4 L=1,3
72 ES(L) = W(L) * CRP
73 ARE(L) =CDSQRT(ES(L) - (HH/ES(L)) - HHH)
74 4 CONTINUE
C TEST(1S -2.0*ARE(1)*ARE(2)*ARE(3)/GGG = 1.0?)
75 GSG = GGG
76 IGSG = AIMAG(GSG)
77 RGSG = REAL(GSG)
78 IF(RGSG)6,5,6
79 5 IF(IGSG)6,9,6
80 6 FN = -2.0*ARE(1)*ARE(2)*ARE(3)/GGG
81 WRITE (6,7) FN
82 7 FORMAT(25X,2HFN/2CX,1P2D19.10//)
83 FNS = FN
84 FNR = REAL(FNS)
85 IF(FNR)8,9,9
86 8 ARE(1) = -ARE(1)
87 9 CONTINUE

```

```

C      SOLUTIONS TO THE BCOCKER QUARTIC
88      Q(1) = ARE(1)+ARE(2)+ARE(3) -BE(3)
89      Q(2) = ARE(1)-ARE(2)-ARE(3) -BE(3)
90      Q(3) =-ARE(1)+ARE(2)-ARE(3) -BE(3)
91      Q(4) =-ARE(1)-ARE(2)+ARE(3) -BE(3)
92      WRITE(6,10) Q(1),Q(2),Q(3),Q(4)
93      10 FORMAT(25X,1HQ/4(2CX,1P2D19.10)/)///)
94      DO 11 LLL=1,4
95      ZERO(LLL) = Q(LLL)*Q(LLL)*Q(LLL)*Q(LLL)+4.0DO*BE(3)*Q(LLL)*Q(LLL)*CHECK
          CQ(LLL)+6.0DO*BE(2)*Q(LLL)*Q(LLL)+4.0DO*BE(1)*Q(LLL) + BE(4) CHECK
96      11 CONTINUE
97      WRITE(6,12)ZERO(1),ZERO(2),ZERO(3),ZERO(4) CHECK
98      12 FORMAT(25X,4HZERO/4(20X,1P2D19.10)/)///) CHECK
99      I = (0.0DC,1.CDO)
C      D SIGNIFIES A DISPERSION MATRIX ELEMENT
C      WE CHOOSE THE SOLUTIONS TO THE QUARTIC EQUATION WHICH CORRESPOND
C      TO UPGOING WAVES, THOSE WITH POSITIVE REAL AND NEGATIVE IMAGINARY PARTS
100     JJ = 1
101     D12 = M(1,2)
102     D32 = M(3,2)
103     D33 = ( CC* CC) + M(3,3)
104     DO 13 KK=1,4
105     QSNGL(KK) = Q(KK)
106     REEL = REAL( QSNGL(KK))
107     IMAG = -AIMAG( QSNGL(KK))
108     IF(.NOT. ( IMAG .GT. 0.0))GO TO 13
109     QUP(JJ) = Q(KK)
110     D11(JJ) = 1.0DC+ M(1,1) -(QUP(JJ)*QUP(JJ))
111     D13(JJ) = M(1,3) + (QUP(JJ)* SS)
112     D31(JJ) = M(3,1) + (QUP(JJ)* SS)
113     DELTA(JJ) = D11(JJ)*D33 - D13(JJ)*D31(JJ)
114     PEEP(JJ) = (-D12*D33 + D13(JJ)*D32)/DELTA(JJ)
115     TEE(JJ) = QUP(JJ)*PEEP(JJ) - (SS*(-D11(JJ)*D32 + D12*D31(JJ)) /
          CDELTA(JJ))
116     JJ = JJ + 1
117     13 CONTINUE
118     WRITE(6,14) QUP(1),QUP(2)
119     14 FORMAT(25X,3HQUP/2(20X,1P2D19.10)/)///)
120     DELT = (TEE(1)* CC + PEEP(1))* ( CC+QUP(2)) - (TEE(2)* CC + PEEP(2)
          C)* ( CC+QUP(1))
121     RC(1) = ((TEE(1)* CC - PEEP(1))* ( CC + QUP(2)) - (TEE(2)* CC -
          CPEEP(2))* ( CC + QUP(1)))/DELT
122     RC(2) =-2.0DO*CC*(QUP(1) - QUP(2))/DELT
123     RC(3) =-2.0DO*CC*(TEE(1)*PEEP(2) - TEE(2)*PEEP(1))/DELT
124     RC(4) = ((TEE(1)* CC + PEEP(1))* ( CC - QUP(2)) - (TEE(2)* CC +
          CPEEP(2))* ( CC - QUP(1)))/DELT
125     DO 15 NN=1,4
126     II=NN+4
127     RSC(NN) = RC(NN)
128     RS(NN)= REAL(RSC(NN))
129     R(NN) = DBLE(RS(NN))
130     RS(II)= AIMAG(RSC(NN))
131     R(II) = DBLE(RS(II))
132     15 CONTINUE
C      R(1)=REAL (PARA R PARA) R(5) = IMAG(PARA R PARA)
C      R(2)=REAL (PARA R PERP) R(6) = IMAG(PARA R PERP)
C      R(3)=REAL (PERP R PARA) R(7) = IMAG(PERP R PARA)
C      R(4)=REAL (PERP R PERP) R(8) = IMAG(PERP R PERP)
133     WRITE(6,40) RC
134     40 FORMAT(28X,18HINITIAL VALUE OF R/4(20X,1P2D18.10/)) CHECK
135     DERR(1) = -(1/2.0DC)*(-T(1,1)+T(4,4)-(T(1,4)/CC)+CC*T(4,1)+RC(1)*
          C(T(1,1)+T(4,4)-(T(1,4)/CC)-CC*T(4,1))+RC(3))*((T(1,2)/CC)-T(4,2))
          C-(T(1,1)+T(4,4)+(T(1,4)/CC)+CC*T(4,1))*RC(1)-(-T(3,1)-(T(3,4)/CC))
          C*RC(2)-RC(1)*RC(1)*(-T(1,1)+T(4,4)+(T(1,4)/CC)-CC*T(4,1))-RC(1)*
          CRC(2)* (T(3,1)-(T(3,4)/CC))-RC(1)*RC(3)*(-T(1,2)/CC)-T(4,2))-RC(2)
          C*RC(3)*(-CC+(T(3,2)/CC))*K
136     DERR(2) =-(1/2.0DO)*((T(1,2)/CC)-T(4,2)+(T(1,1)+T(4,4)-(T(1,4)/CC)
          C-CC*T(4,1))*RC(2)+((T(1,2)/CC)-T(4,2))*RC(4)-(-T(1,2)/CC)-T(4,2))
          C*RC(1)-(CC+(T(3,2)/CC))*RC(2)-RC(1)*RC(2)*(-T(1,1)+T(4,4)+(T(1,4)/
          CCC)-CC*T(4,1))-RC(2)*RC(2)* (T(3,1)-(T(3,4)/CC))-RC(1)*RC(4)*(-T(1
          C,2)/CC)-T(4,2))-RC(2)*RC(4)*(-CC+(T(3,2)/CC))*K

```

```

137      DERR(3) = -(I/2.0DC)*(T(3,1)+(T(3,4)/CC)+(-T(3,1)+(T(3,4)/CC))*RC
C(1) +(-CC-(T(3,2)/CC))*RC(3) -RC(3)*(T(1,1)+T(4,4)+(T(1,4)/CC)+
CCC*T(4,1)) -RC(4)*(-T(3,1)-(T(3,4)/CC)) -RC(1)*RC(3)*(-T(1,1)+
CT(4,4)+(T(1,4)/CC)-CC*T(4,1)) -RC(1)*RC(4)*(T(3,1)-(T(3,4)/CC))
C-RC(3)*RC(3)*(-T(1,2)/CC)-T(4,2)) -RC(3)*RC(4)*(-CC+(T(3,2)/CC)))
C *K
138      DERR(4) = -(I/2.0DC)*(CC-(T(3,2)/CC)+RC(2)*(-T(3,1)+(T(3,4)/CC))
C+RC(4)*(-CC-(T(3,2)/CC)) -RC(3)*(-T(1,2)/CC)-T(4,2)) -RC(4)*(CC+
C(T(3,2)/CC)) -RC(2)*RC(3)*(-T(1,1)+T(4,4)+(T(1,4)/CC)-CC*T(4,1))
C-RC(2)*RC(4)*(T(3,1) -(T(3,4)/CC)) -RC(3)*RC(4)*(-T(1,2)/CC)-T(4,
C2)) -RC(4)*RC(4)*(-CC+(T(3,2)/CC))) *K
139      WRITE(6,33) DERR
140      33 FORMAT(28X,21HINITIAL VALUE OF DERR/4(20X,1P2D18.10//)
141      MAGR(1) = DSQRT((R(1)**2) + (R(5)**2))
142      MAGR(2) = DSQRT((R(2)**2) + (R(6)**2))
143      MAGR(3) = DSQRT((R(3)**2) + (R(7)**2))
144      MAGR(4) = DSQRT((R(4)**2) + (R(8)**2))
145      FAZR(1) = DATAN(R(5)/R(1))*180.0/PI
146      FAZR(2) = DATAN(R(6)/R(2))*180.0/PI
147      FAZR(3) = DATAN(R(7)/R(3))*180.0/PI
148      FAZR(4) = DATAN(R(8)/R(4))*180.0/PI
149      WRITE(6,16)
150      16 FORMAT(//25X,32HSTARTING REFLECTION COEFFICIENTS//27X,4HMAGR,14X,
C4HFAZR//)
151      WRITE(6,17)MAGR(1),FAZR(1),MAGR(2),FAZR(2),MAGR(3),FAZR(3),
CMAGR(4),FAZR(4)
152      17 FORMAT(4(20X,1P2D19.10//)
153      RPOLY = ((( RC(1) - 1.0D0)/2.0D0)*(( RC(4) + 1.0D0)/2.0D0) -
C(RC(3)/2.0D0)*(( RC(2)/2.0D0))
154      AM(1) = -((( RC(4) + 1.0D0)/(2.0D0 * RPOLY)) + 1.0D0)/CC
155      AM(2) = - RC(2)/(2.0D0*RPOLY)
156      AM(3) = - RC(3)/(2.0D0*RPOLY)
157      AM(4) = -((( RC(1) - 1.0D0)/(2.0D0 * RPOLY)) - 1.0D0) * CC
158      DO 18 MM=1,4
159      LL=MM + 4
160      AMS(MM) = AM(MM)
161      YS(MM) = REAL(AMS(MM))
162      Y(MM) = DBLE(YS(MM))
163      YS(LL) = AIMAG(AMS(MM))
164      Y(LL) = DBLE(YS(LL))
165      18 CONTINUE
C      Y(1) =REAL (A11)      Y(5) = IMAG (A11)
C      Y(2) =REAL (A12)      Y(6) = IMAG (A12)
C      Y(3) =REAL (A21)      Y(7) = IMAG (A21)
C      Y(4) =REAL (A22)      Y(8) = IMAG (A22)
166      WRITE(6,19)
167      19 FORMAT(//30X,18HINITIAL VALUE OF Y/27X,5HREALY,14X,5HIMAGY//)
168      WRITE(6,20) AM
169      20 FORMAT(4(20X,1P2D19.10//)
170      DERIV(1) =(-I*(T(4,4)*AM(1) -T(1,1)*AM(1) +T(4,1) +AM(2)*AM(3) CHECK
C -T(1,4)*AM(1)*AM(1)))*K CHECK
171      DERIV(2) =(-I*(T(4,4)*AM(2) +T(1,2)*AM(2) -T(4,2) +AM(2)*AM(4) CHECK
C -T(1,4)*AM(1)*AM(2)))*K CHECK
172      DERIV(3) =(-I*(-T(1,1)*AM(3) +T(3,4)*AM(1) +T(3,1) +AM(3)*AM(4) CHECK
C -T(1,4)*AM(1)*AM(3)))*K CHECK
173      DERIV(4) =(-I*(T(1,2)*AM(3) +T(3,4)*AM(2) -T(3,2) +AM(4)*AM(4) CHECK
C -T(1,4)*AM(2)*AM(3)))*K CHECK
174      WRITE(6,22) CHECK
175      22 FORMAT(//28X,21HINITIAL VALUE OF DERY/24X,8HREALDERY,14X,8HIMAGDECHECK
CRY//) CHECK
176      WRITE(6,23) DERIV
177      23 FORMAT(20X,1P2D19.10/20X,1P2D19.10/20X,1P2D19.10/20X,1P2D19.10//) CHECK
C      END CALCULATION OF INITIAL SOLUTIONS.
178      24 DERY(1) = .1250D0
179      DERY(2) = .1250D0
180      DERY(3) = .1250D0
181      DERY(4) = .1250D0
182      DERY(5) = .1250D0
183      DERY(6) = .1250D0
184      DERY(7) = .1250D0
185      DERY(8) = .1250D0

```

```

C      ASSOCIATE ALTITUDES WITH ED AND CF DATA POINTS.
186      NMAXI = NMAX + 1
187      DO 32 J=1,NMAXI
188      ALT(J) = PRMT(1) + (PRMT(3)*(J-1))
189      32 CONTINUE
C      IT MUST BE REMEMBERED THAT THE INDEPENDENT VARIABLE X IN THIS
C      PROGRAM REPRESENTS Z OR H , THE ALTITUDE , NOT THE X
C      DIRECTION, THAT THE DEPENDENT VARIABLE Y REPRESENTS THE
C      ADMITTANCE MATRIX A, NOT THE Y DIRECTION, AND THAT Z IS
C      CF(N) / OMEGA, NOT THE Z(OR H OR VERTICAL) DIRECTION.
C      THIS IS CONFUSING NOTATION BUT ELIMINATES THE NECESSITY TO
C      CHANGE VARIABLE NAMES IN THE DRKGS SUBROUTINE.
C      THE INTEGRATION IS STARTED ARBITRARILY WHERE EX= 100 * ( 1 + WHY)
C      , I.E., WELL ABOVE THE HEIGHT OF REFLECTIONS, AND CONTINUES DOWN TO
C      LEVELS WHERE N < 1 ELECTRON/CM**3
C      BEGIN CALCULATIONS OF FINAL SOLUTIONS.
190      CALL DRKGS (PRMT,Y, DERY,NDIM,IHLF,FCI,OUTP,AUX,ALT, X, TR,II,
CMR,MI,R,CC,DCL,DCM,DCN,WHY,SS,ED,CF,OMEGA,ELECM,PERME,E,K,ZDATA)
191      YPOLYR=-1.000 -(CC*Y(1)) +(Y(4)/CC)+Y(1)*Y(4) -Y(5)*Y(8) -Y(2)*Y(3
C) +Y(6)*Y(7)
192      YPOLYI= -CC*Y(5) +(Y(8)/CC) +Y(1)*Y(8) +Y(4)*Y(5) -Y(2)*Y(7)
C-Y(3)*Y(6)
193      YDENOM = (YPOLYR**2) + (YPOLYI**2)
194      R(1) =(2.000 * (YPOLYR*(1.000-(Y(4)/CC))-(Y(8)*YPOLYI/CC))/YDENOM
C)+ 1.000
195      R(2)= -2.000*(Y(2)*YPOLYR +Y(6)*YPOLYI)/YDENOM
196      R(3)= -2.000*(Y(3)*YPOLYR +Y(7)*YPOLYI)/YDENOM
197      R(4) = (-2.000*(YPOLYR*(CC*Y(1) + 1.000) + YPOLYI * CC*Y(5))/
CYDENOM) - 1.000
198      R(5) = (-2.000*(YPOLYI*(1.000 - (Y(4)/CC)) + YPOLYR*(Y(8)/CC))/
CYDENOM)
199      R(6)=-2.000*(-Y(2)*YPOLYI +Y(6)*YPOLYR)/YDENOM
200      R(7)=-2.000*(-Y(3)*YPOLYI +Y(7)*YPOLYR)/YDENOM
201      R(8) = 2.000*(-YPOLYR*CC*Y(5) + YPOLYI*(CC*Y(1)+1.000))/YDENOM
202      DO 46 LA=1,4
203      LO = LA + 4
204      MAGR(LA) = DSQRT((R(LA)*R(LA)) + (R(LO)*R(LO)))
205      FAZR(LA) = (DATAN(DABS(R(LO)/R(LA))))*180.0/PI
206      IF(R(LO))41,43,43
207      41 IF(R(LA))42,45,45
208      42 FAZR(LA) = FAZR(LA) + 180.0
209      GOTO 46
210      43 IF(R(LA))44,46,46
211      44 FAZR(LA) = FAZR(LA) + 90.0
212      GOTO 46
213      45 FAZR(LA) = FAZR(LA) + 270.0
214      46 CONTINUE
215      WRITE(6,26)
216      26 FORMAT(//7X,1HX,8X,4HIHLF,7X,5HREALY,14X,5HIMAGY,12X,8HREALDERY,
C11X,8HIMAGDERY,13X,5HREALR,14X,5HIMAGR/19X,1HN/)
217      WRITE(6,27)X,IHLF,Y(1),Y(5),DERY(1),DERY(5),R(1),R(5),Y(2),Y(6),
CDERY(2),DERY(6),R(2),R(6),Y(3),Y(7),DERY(3),DERY(7),R(3),R(7),
CY(4),Y(8),DERY(4),DERY(8),R(4),R(8),N
218      27 FORMAT(1X,1P1D16.10,13,1P6D18.10/20X,1P6D18.10/20X,1P6D18.10/
C20X,1P6D18.10/20//)
219      WRITE(6,28)MAGR(1),FAZR(1),MAGR(2),FAZR(2),MAGR(3),FAZR(3),
CMAGR(4),FAZR(4)
220      28 FORMAT(/////30X,35HFINAL REFLECTION COEFFICIENT VALUES//36X,
C4HMAGR,18X,4HFAZR//15X,5H1R11,5X,1P2D22.10/15X,5H1R +,5X,
C1P2D22.10/15X,5H+ R11,5X,1P2D22.10/15X,5H+ R +,5X,1P2D22.10)
221      29 STOP
222      END

```

```

223 SUBROUTINE PREFN(M,T ,SS,CC,DCL,DCM,DCN,EDPRE,CFPRE,OMEGA,ELECM,
      CPERME,E,K,B)
224 DIMENSION M(2,3)
      C,T(4,4) CHECK
225 REAL*8 SS,CC,DCL,DCM,DCN,EDPRE,CFPRE,OMEGA,ELECM,PERME,E,K,
      CB,EX,WHY,Z
226 COMPLEX*16 M,U,COEFF,I
      C,T,UNDER CHECK
      C CALCULATIONS ARE DONE IN COMPLEX NUMBERS.
227 EX = EDPRE*E*E/(PERME*ELECM*OMEGA*OMEGA)
228 WHY = -E*B/(OMEGA*ELECM)
229 Z = CFPRE/OMEGA
      C U = UR + I * UI
230 I = (0.0D0,1.0D0)
231 U = 1.0D0 - I * Z
232 COEFF = -EX/(U*(U*U-WHY*WHY))
233 M(1,1) = COEFF*(U*U - DCL*DCL*WHY*WHY)
234 M(1,2) = COEFF*(-I*U*DCN*WHY - DCL*DCM*WHY*WHY)
235 M(1,3) = COEFF*(I*L*DCM*WHY - DCL*DCN*WHY*WHY)
236 M(2,1) = COEFF*(I*U*DCN*WHY - DCL*DCM*WHY*WHY)
237 M(2,2) = COEFF*(U*U - DCM*DCM*WHY*WHY)
238 M(2,3) = COEFF*(-I*U*DCL*WHY - DCM*DCN*WHY*WHY)
239 M(3,1) = COEFF*(-I*U*DCM*WHY - DCL*DCN*WHY*WHY)
240 M(3,2) = COEFF*(I*L*DCL*WHY - DCM*DCN*WHY*WHY)
241 M(3,3) = COEFF*(U*U - DCN*DCN*WHY*WHY)
242 UNDER = 1.0D0 + M(3,3) CHECK
243 T(1,1) = -SS*M(3,1)/UNDER CHECK
244 T(1,2) = SS*M(3,2)/UNDER CHECK
245 T(1,3) = (0.0D0,0.0D0) CHECK
246 T(1,4) = ((CC*CC) + M(3,3))/UNDER CHECK
247 T(2,1) = (0.0D0,0.0D0) CHECK
248 T(2,2) = (0.0D0,0.0D0) CHECK
249 T(2,3) = (1.0D0,0.0D0) CHECK
250 T(2,4) = (0.0D0,0.0D0) CHECK
251 T(3,1) = (M(2,3)*M(3,1)/UNDER) - M(2,1) CHECK
252 T(3,2) = (CC*CC) + M(2,2) - (M(2,3)*M(3,2)/UNDER) CHECK
253 T(3,3) = (0.0D0,0.0D0) CHECK
254 T(3,4) = SS*M(2,3)/UNDER CHECK
255 T(4,1) = 1.0D0 + M(1,1) - (M(1,3)*M(3,1)/UNDER) CHECK
256 T(4,2) = (M(3,2)*M(1,3)/UNDER) - M(1,2) CHECK
257 T(4,3) = (0.0D0,0.0D0) CHECK
258 T(4,4) = -SS*M(1,3)/UNDER CHECK
259 WRITE(6,41)M(1,1),M(1,2),M(1,3),M(2,1),M(2,2),M(2,3),M(3,1),
      CM(3,2),M(3,3) CHECK
260 41 FORMAT(40X,16HM(COMPLEX CALC.)/3(2X,1P2D18.10,2X,1P2D18.10,2X,
      C1P2D18.10/)) CHECK
261 WRITE(6,42)T(1,1),T(1,2),T(1,3),T(1,4),T(2,1),T(2,2),T(2,3),
      CT(2,4),T(3,1),T(3,2),T(3,3),T(3,4),T(4,1),T(4,2),T(4,3),T(4,4) CHECK
262 42 FORMAT(40X,16HT(COMPLEX CALC.)/4(2X,1P2D13.5,2X,1P2D13.5,2X,
      C1P2D13.5,2X,1P2D13.5/)) CHECK
263 RETURN
264 END

```



```

265      SUBROUTINE FCT(X,Y,DERY,TR,TI,MR,MI,SS,CC,DCL,DCM,DCN,ED,CF,OMEGA,
        CELECM,PERME,E,K,ALT,PRMT,N,EVE,ZDATA)
266      DIMENSION Y(8),DERY(8),TR(4,4),TI(4,4),MR(3,3),MI(3,3),PRMT(5),
        CED(119),CF(119),ALT(120)
267      REAL*8 X,Y,DERY,TR,TI,MR,MI,SS,CC,DCL,DCM,DCN,ED,CF,OMEGA,ELECM,
        CPERME,E,K,B,EX,WHY,Z,UR,UI,UPOLYR,UPOLYI,UDENOM,MDENOM,DABS
        C,ALT,EDENS,PRMT,EVE,ZDATA,CFREQ
        C      CALCULATIONS ARE DONE IN REAL NUMBERS- COMPLEX NUMBERS SEPARATED
        C      INTO REAL AND IMAGINARY PARTS.
        C      BETWEEN ALTITUDES FOR WHICH ED AND CF HAVE BEEN SPECIFIED ON DATA CARDS
        C      CED AND CF ARE LINEARLY INTERPOLATED.
268      N = -((PRMT(1)-X)/ZDATA) + 1
269      L = N + 1
270      EDENS = -((ALT(N)-X)*ED(L)/ZDATA) + (ALT(L)-X)*ED(N)/ZDATA
271      CFREQ = -((ALT(N)-X)*CF(L)/ZDATA) + (ALT(L)-X)*CF(N)/ZDATA
272      IF(EVE-EDENS)47,46,47
273      47 EVE = EDENS
274      B = C.560D-4
        C      EX IS DIMENSIONLESS AND IS THE RATIO OF THE SQUARE OF THE PLASMA
        C      FREQUENCY TO THE SQUARE OF THE WAVE FREQUENCY
        C      PERMM IS NOT INCLUDED IN WHY IN MKS UNITS, WHY IS DIMENSIONLESS
        C      AND IS THE RATIO OF THE GYROFREQUENCY TO THE WAVE FREQUENCY
        C      Z IS DIMENSIONLESS AND IS THE RATIO OF THE COLLISION FREQUENCY
        C      TO THE WAVE ANGULAR VELOCITY(OR 2*PI*WAVE FREQUENCY)
275      EX = EDENS*E*E/(PERME*ELECM*OMEGA*OMEGA)
276      WHY = DABS(E*B/(OMEGA*ELECM))
277      Z = CFREQ/OMEGA
        C      U = UR + I * UI
278      UR = 1.0
279      UI = -Z
        C      UPOLY = UPOLYR + I * UPOLYI
280      UPOLYR = (UR**3) - (3.CD0*UR*(UI**2)) - (UR * (WHY**2))
281      UPOLYI = -(UI**2) + (3.CD0*UI*(UR**2)) - (UI * (WHY**2))
282      UDENOM = UPOLYR**2 + UPOLYI**2
        C      M = MR + I * MI
283      MR(1,1)=-EX*((UPOLYR*((UR**2)-(UI**2)-((DCL**2)*(WHY**2))))+(
        CUPOLYI*2.0D0*UI*UR))/UDENOM
284      MI(1,1)=-EX*((UPOLYR*2.0D0*UI*UR)-(UPOLYI*((UR**2)-(UI**2)-((DCL**
        C2)*(WHY**2)))))/UDENOM
285      MR(1,2)=EX*((UPOLYR*((DCL*DCM*(WHY**2))-(UI*DCN*WHY)))+(UPOLYI*UR*
        CDCN*WHY))/UDENOM
286      MI(1,2)=EX*((UPOLYI*((UI*DCN*WHY)-(DCL*DCM*(WHY**2))))+(UPOLYR*UR*
        CDCN*WHY))/UDENOM
287      MR(1,3)=EX*((UPOLYR*((DCL*DCN*(WHY**2))+(UI*DCM*WHY)))-(UPOLYI*UR*
        CDCM*WHY))/UDENOM
288      MI(1,3)=EX*((UPOLYI*((UI*DCM*WHY)+(DCL*DCN*(WHY**2))))+(UPOLYR*UR*
        CDCM*WHY))/(-UDENOM)
289      MR(2,1)=EX*((UPOLYR*((DCL*DCM*(WHY**2))+(UI*DCN*WHY)))-(UPOLYI*UR*
        CDCN*WHY))/UDENOM
290      MI(2,1)=EX*((UPOLYI*((UI*DCN*WHY)+(DCL*DCM*(WHY**2))))+(UPOLYR*UR*
        CDCN*WHY))/(-UDENOM)
291      MR(2,2)=-EX*((UPOLYR*((UR**2)-(UI**2)-((DCM**2)*(WHY**2))))+(
        CUPOLYI*2.0D0*UI*UR))/UDENOM
292      MI(2,2)=-EX*((UPOLYR*2.0D0*UI*UR)-(UPOLYI*((UR**2)-(UI**2)-((DCM**
        C2)*(WHY**2)))))/UDENOM
293      MR(2,3)=EX*((UPOLYR*((DCN*DCM*(WHY**2))-(UI*DCL*WHY)))+(UPOLYI*UR*
        CCCL*WHY))/UDENOM
294      MI(2,3)=EX*((UPOLYI*((UI*DCL*WHY)-(DCN*DCM*(WHY**2))))+(UPOLYR*UR*
        CDCL*WHY))/UDENOM
295      MR(3,1)=EX*((UPOLYR*((DCL*DCN*(WHY**2))-(UI*DCM*WHY)))+(UPOLYI*UR*
        CDCM*WHY))/UDENOM
296      MI(3,1)=EX*((UPOLYI*((UI*DCM*WHY)-(DCL*DCN*(WHY**2))))+(UPOLYR*UR*
        CDCM*WHY))/UDENOM
297      MR(3,2)=EX*((UPOLYR*((DCM*DCN*(WHY**2))+(UI*DCL*WHY)))-(UPOLYI*UR*
        CDCL*WHY))/UDENOM
298      MI(3,2)=EX*((UPOLYI*((UI*DCL*WHY)+(DCM*DCN*(WHY**2))))+(UPOLYR*UR*
        CDCL*WHY))/(-UDENOM)
299      MR(3,3)=-EX*((UPOLYR*((UR**2)-(UI**2)-((DCN**2)*(WHY**2))))+(
        CUPOLYI*2.0D0*UI*UR))/UDENOM
300      MI(3,3)=-EX*((UPOLYR*2.0D0*UI*UR)-(UPOLYI*((UR**2)-(UI**2)-((DCN**
        C2)*(WHY**2)))))/UDENOM
301      MDENOM = ((1.0D0 + MR(3,3))**2) + (MI(3,3)**2)
        C      T = TR + I * TI
302      TR(1,1)=-((SS*((MR(3,1)*(1.0D0+MR(3,3)))+(MI(3,1)*MI(3,3))))/MDENOM
303      TI(1,1)=-((SS*((-MR(3,1)*MI(3,3))+(MI(3,1)*(1.0D0+MR(3,3)))))/MDENO
        CM

```

```

304 TR(1,2)={SS*{(MR(3,2)*(1.000+MR(3,3)))+(MI(3,2)*MI(3,3))}/MDENOM
305 TI(1,2)={SS*{(-MR(3,2)*MI(3,3))+(MI(3,2)*(1.000+MR(3,3)))}/MDENOM
CM
306 TR(1,3)=0.000
307 TI(1,3)=0.000
308 TR(1,4)={((CC**2)+MR(3,3))*(1.000+MR(3,3))+(MI(3,3)**2)}/MDENOM
309 TI(1,4)={MI(3,3)*(1.000+MR(3,3))-MI(3,3)*((CC**2)+MR(3,3))}/MDENOM
310 TR(2,1)=0.000
311 TI(2,1)=0.000
312 TR(2,2)=0.000
313 TI(2,2)=0.000
314 TR(2,3)=1.000
315 TI(2,3)=0.000
316 TR(2,4)=0.000
317 TI(2,4)=0.000
318 TR(3,1)={MR(2,3)*MR(3,1)*(1.000+MR(3,3))-MI(2,3)*MI(3,1)*(1.000+
CMR(3,3))+MR(2,3)*MI(3,1)*MI(3,3)+MR(3,1)*MI(2,3)*MI(3,3)}/MDENOM
C-MR(2,1)
319 TI(3,1)={MI(2,3)*MI(3,1)*MI(3,3)-MR(2,3)*MR(3,1)*MI(3,3)+MR(2,3)*
C(1.000+MR(3,3))*MI(3,1)+MI(2,3)*MR(3,1)*(1.000+MR(3,3))}/MDENOM
C-MI(2,1)
320 TR(3,2)={MR(3,2)*MR(2,3)*(1.000+MR(3,3))-MI(3,2)*MI(2,3)*(1.000+
CMR(3,3))+MR(3,2)*MI(2,3)*MI(3,3)+MR(2,3)*MI(3,2)*MI(3,3)}/(-MDENOM
C)+((CC**2)+MR(2,2)
321 TI(3,2)={MI(3,2)*MI(2,3)*MI(3,3)-MR(3,2)*MR(2,3)*MI(3,3)+MR(3,2)*
C(1.000+MR(3,3))*MI(2,3)+MI(3,2)*MR(2,3)*(1.000+MR(3,3))}/(-MDENOM
C)+MI(2,2)
322 TR(3,3)=0.000
323 TI(3,3)=0.000
324 TR(3,4)={SS*{(MR(2,3)*(1.000+MR(3,3)))+(MI(2,3)*MI(3,3))}/MDENOM
325 TI(3,4)={SS*{(-MR(2,3)*MI(3,3))+(MI(2,3)*(1.000+MR(3,3)))}/MDENOM
CM
326 TR(4,1)={MR(3,1)*MR(1,3)*(1.000+MR(3,3))-MI(3,1)*MI(1,3)*(1.000+
CMR(3,3))+MR(3,1)*MI(1,3)*MI(3,3)+MR(1,3)*MI(3,1)*MI(3,3)}/(-MDENOM
C)+1.000+MR(1,1)
327 TI(4,1)={MI(3,1)*MI(1,3)*MI(3,3)-MR(3,1)*MR(1,3)*MI(3,3)+MR(3,1)*
C(1.000+MR(3,3))*MI(1,3)+MI(3,1)*MR(1,3)*(1.000+MR(3,3))}/(-MDENOM
C)+MI(1,1)
328 TR(4,2)={MR(3,2)*MR(1,3)*(1.000+MR(3,3))-MI(3,2)*MI(1,3)*(1.000+
CMR(3,3))+MR(3,2)*MI(1,3)*MI(3,3)+MR(1,3)*MI(3,2)*MI(3,3)}/MDENOM
C-MR(1,2)
329 TI(4,2)={MI(3,2)*MI(1,3)*MI(3,3)-MR(3,2)*MR(1,3)*MI(3,3)+MR(3,2)*
C(1.000+MR(3,3))*MI(1,3)+MI(3,2)*MR(1,3)*(1.000+MR(3,3))}/MDENOM
C-MI(1,2)
330 TR(4,3)=0.000
331 TI(4,3)=0.000
332 TR(4,4)={SS*{(MR(1,3)*(1.000+MR(3,3)))+(MI(1,3)*MI(3,3))}/MDENOM
333 TI(4,4)={SS*{(-MR(1,3)*MI(3,3))+(MI(1,3)*(1.000+MR(3,3)))}/MDENOM
CM
334 46 DERY(1)={-TR(1,1)*Y(5)-TI(1,1)*Y(1)+TR(4,4)*Y(5)+TI(4,4)*Y(1)
C-2.000*Y(1)*Y(5)*TR(1,4)-(Y(1)**2)*TI(1,4)+(Y(5)**2)*TI(1,4)
C+Y(2)*Y(7)+Y(6)*Y(3)+TI(4,1)*K
335 DERY(2)={TI(1,2)*Y(1)+TR(1,2)*Y(5)+TI(4,4)*Y(2)+TR(4,4)*Y(6)
C-Y(1)*Y(2)*TI(1,4)-Y(1)*Y(6)*TR(1,4)-Y(2)*Y(5)*TR(1,4)
C+Y(2)*Y(8)+Y(4)*Y(6)+Y(5)*Y(6)*TI(1,4)-TI(4,2)*K
336 DERY(3)={-TR(1,1)*Y(7)-TI(1,1)*Y(3)+TR(3,4)*Y(5)+TI(3,4)*Y(1)
C-Y(1)*Y(3)*TI(1,4)-Y(5)*Y(3)*TR(1,4)-Y(7)*Y(1)*TR(1,4)+TI(3,1)
C+Y(5)*Y(7)*TI(1,4)+Y(3)*Y(8)+Y(7)*Y(4)*K
337 DERY(4)={TR(1,2)*Y(7)+TI(1,2)*Y(3)+TR(3,4)*Y(6)+TI(3,4)*Y(2)
C-Y(2)*Y(3)*TI(1,4)-Y(6)*Y(3)*TR(1,4)-Y(2)*Y(7)*TR(1,4)-TI(3,2)
C+Y(6)*Y(7)*TI(1,4)+2.000*Y(4)*Y(8)*K
338 DERY(5)={TR(1,1)*Y(1)-TI(1,1)*Y(5)-TR(4,4)*Y(1)+TI(4,4)*Y(5)
C+(Y(1)**2)*TR(1,4)-(Y(5)**2)*TR(1,4)-2.000*Y(1)*Y(5)*TI(1,4)
C-Y(2)*Y(3)+Y(6)*Y(7)-TR(4,1)*K
339 DERY(6)={-TR(1,2)*Y(1)+TI(1,2)*Y(5)-TR(4,4)*Y(2)+TI(4,4)*Y(6)
C+Y(1)*Y(2)*TR(1,4)-Y(5)*Y(6)*TR(1,4)-TI(1,4)*Y(6)*Y(1)+TR(4,2)
C-TI(1,4)*Y(5)*Y(2)-Y(2)*Y(4)+Y(6)*Y(8)*K
340 DERY(7)={TR(1,1)*Y(3)-TI(1,1)*Y(7)-TR(3,4)*Y(1)+TI(3,4)*Y(5)
C+Y(1)*Y(3)*TR(1,4)-Y(5)*Y(7)*TR(1,4)-Y(1)*Y(7)*TI(1,4)-TR(3,1)
C-Y(3)*Y(5)*TI(1,4)-Y(3)*Y(4)+Y(7)*Y(8)*K
341 DERY(8)={-TR(1,2)*Y(3)+TI(1,2)*Y(7)-TR(3,4)*Y(2)+TI(3,4)*Y(6)
C+Y(2)*Y(3)*TR(1,4)-Y(6)*Y(7)*TR(1,4)-Y(2)*Y(7)*TI(1,4)+TR(3,2)
C-Y(6)*Y(3)*TI(1,4)-(Y(4)**2)+(Y(8)**2)*K
342 RETURN
343 END

```

```

344 SUBROUTINE OUTP (X, Y, DERY, IHLF, NDIM, PRMT, N, R, CC)
345 DIMENSION Y(8), DERY(8), PRMT(5), R(8)
346 REAL*8 X, PRMT, Y, DERY, R, YPOLYR, YPOLYI, YDENOM, DABS, CC
C YPOLY = YPOLYR + I * YPOLYI
347 YPOLYR = -1.000 - (CC*Y(1)) + (Y(4)/CC) + Y(1)*Y(4) - Y(5)*Y(8) - Y(2)*Y(3)
C) + Y(6)*Y(7)
348 YPOLYI = -CC*Y(5) + (Y(8)/CC) + Y(1)*Y(8) + Y(4)*Y(5) - Y(2)*Y(7)
C - Y(3)*Y(6)
349 YDENOM = (YPOLYR**2) + (YPOLYI**2)
350 R(1) = (2.000 * (YPOLYR*(1.000 - (Y(4)/CC)) - (Y(8)*YPOLYI/CC)))/YDENOM
C) + 1.000
351 R(2) = -2.000*(Y(2)*YPOLYR + Y(6)*YPOLYI)/YDENOM
352 R(3) = -2.000*(Y(3)*YPOLYR + Y(7)*YPOLYI)/YDENOM
353 R(4) = (-2.000*(YPOLYR*(CC*Y(1) + 1.000) + YPOLYI * CC*Y(5)))/
CYDENOM) - 1.000
354 R(5) = (-2.000*(YPOLYI*(1.000 - (Y(4)/CC)) + YPOLYR*(Y(8)/CC))/
CYDENOM)
355 R(6) = -2.000*(-Y(2)*YPOLYI + Y(6)*YPOLYR)/YDENOM
356 R(7) = -2.000*(-Y(3)*YPOLYI + Y(7)*YPOLYR)/YDENOM
357 R(8) = 2.000*(-YPOLYR*CC*Y(5) + YPOLYI*(CC*Y(1)+1.000))/YDENOM
358 8 WRITE(6,9) X, IHLF, Y(1), Y(5), DERY(1), DERY(5), R(1), R(5), Y(2), Y(6), CHECK
C DERY(2), DERY(6), R(2), R(6), Y(3), Y(7), DERY(3), DERY(7), R(3), R(7), CHECK
C Y(4), Y(8), DEPY(4), DERY(8), R(4), R(8), N CHECK
359 9 FORMAT(1X, 1P1D16.10, I3, 1P6D18.10/20X, 1P6D18.10/20X, 1P6D18.10/ CHECK
C 20X, 1P6D18.10/I20//) CHECK
360 12 RETURN
361 END
C DRKGS001
C ..... DRKGS002
C DRKGS003
C SUBROUTINE DRKGS DRKGS004
C DRKGS005
C PURPOSE DRKGS006
C TO SOLVE A SYSTEM OF FIRST ORDER ORDINARY DIFFERENTIAL DRKGS007
C EQUATIONS WITH GIVEN INITIAL VALUES. DRKGS008
C DRKGS009
C USAGE DRKGS010
C CALL DRKGS (PRMT, Y, DERY, NDIM, IHLF, FCT, OUTP, AUX) DRKGS011
C PARAMETERS FCT AND OUTP REQUIRE AN EXTERNAL STATEMENT. DRKGS012
C DRKGS013
C DESCRIPTION OF PARAMETERS DRKGS014
C PRMT - DOUBLE PRECISION INPUT AND OUTPUT VECTOR WITH DRKGS015
C DIMENSION GREATER THAN OR EQUAL TO 5, WHICH DRKGS016
C SPECIFIES THE PARAMETERS OF THE INTERVAL AND OF DRKGS017
C ACCURACY AND WHICH SERVES FOR COMMUNICATION BETWEEN DRKGS018
C OUTPUT SUBROUTINE (FURNISHED BY THE USER) AND DRKGS019
C SUBROUTINE DRKGS. EXCEPT PRMT(5) THE COMPONENTS DRKGS020
C ARE NOT DESTROYED BY SUBROUTINE DRKGS AND THEY ARE DRKGS021
C PRMT(1)- LOWER BOUND OF THE INTERVAL (INPUT), DRKGS022
C PRMT(2)- UPPER BOUND OF THE INTERVAL (INPUT), DRKGS023
C PRMT(3)- INITIAL INCREMENT OF THE INDEPENDENT VARIABLE DRKGS024
C (INPUT), DRKGS025
C PRMT(4)- UPPER ERROR BOUND (INPUT). IF ABSOLUTE ERROR IS DRKGS026
C GREATER THAN PRMT(4), INCREMENT GETS HALVED. DRKGS027
C IF INCREMENT IS LESS THAN PRMT(3) AND ABSOLUTE DRKGS028
C ERROR LESS THAN PRMT(4)/50, INCREMENT GETS DOUBLED. DRKGS029
C THE USER MAY CHANGE PRMT(4) BY MEANS OF HIS DRKGS030
C OUTPUT SUBROUTINE. DRKGS031
C PRMT(5)- NO INPUT PARAMETER. SUBROUTINE DRKGS INITIALIZES DRKGS032
C PRMT(5)=0. IF THE USER WANTS TO TERMINATE DRKGS033
C SUBROUTINE DRKGS AT ANY OUTPUT POINT, HE HAS TO DRKGS034
C CHANGE PRMT(5) TO NON-ZERO BY MEANS OF SUBROUTINE DRKGS035
C OUTP. FURTHER COMPONENTS OF VECTOR PRMT ARE DRKGS036
C FEASIBLE IF ITS DIMENSION IS DEFINED GREATER DRKGS037
C THAN 5. HOWEVER SUBROUTINE DRKGS DOES NOT REQUIRE DRKGS038
C AND CHANGE THEM. NEVERTHELESS THEY MAY BE USEFUL DRKGS039
C FOR HANDING RESULT VALUES TO THE MAIN PROGRAM DRKGS040
C (CALLING DRKGS) WHICH ARE OBTAINED BY SPECIAL DRKGS041
C MANIPULATIONS WITH OUTPUT DATA IN SUBROUTINE OUTP. DRKGS042
C Y - DOUBLE PRECISION INPUT VECTOR OF INITIAL VALUES DRKGS043
C (DESTROYED). LATERON Y IS THE RESULTING VECTOR OF DRKGS044

```

C		DEPENDENT VARIABLES COMPUTED AT INTERMEDIATE	DRKGS045
C		POINTS X.	DRKGS046
C	DERY	- DOUBLE PRECISION INPUT VECTOR OF ERROR WEIGHTS	DRKGS047
C		(DESTROYED). THE SUM OF ITS COMPONENTS MUST BE	DRKGS048
C		EQUAL TO 1. LATERON DERY IS THE VECTOR OF	DRKGS049
C		DERIVATIVES, WHICH BELONG TO FUNCTION VALUES Y AT	DRKGS050
C		INTERMEDIATE POINTS X.	DRKGS051
C	NDIM	- AN INPUT VALUE, WHICH SPECIFIES THE NUMBER OF	DRKGS052
C		EQUATIONS IN THE SYSTEM.	DRKGS053
C	IHLF	- AN OUTPUT VALUE, WHICH SPECIFIES THE NUMBER OF	DRKGS054
C		BISECTIONS OF THE INITIAL INCREMENT. IF IHLF GETS	DRKGS055
C		GREATER THAN 10, SUBROUTINE DRKGS RETURNS WITH	DRKGS056
C		ERROR MESSAGE IHLF=11 INTO MAIN PROGRAM. ERROR	DRKGS057
C		MESSAGE IHLF=12 OR IHLF=13 APPEARS IN CASE	DRKGS058
C		PRMT(3)=0 OR IN CASE SIGN(PRMT(3)).NE.SIGN(PRMT(2)-	DRKGS059
C		PRMT(1)) RESPECTIVELY.	DRKGS060
C	FCT	- THE NAME OF AN EXTERNAL SUBROUTINE USED. THIS	DRKGS061
C		SUBROUTINE COMPUTES THE RIGHT HAND SIDES DERY OF	DRKGS062
C		THE SYSTEM TO GIVEN VALUES X AND Y. ITS PARAMETER	DRKGS063
C		LIST MUST BE X,Y,DERY. SUBROUTINE FCT SHOULD	DRKGS064
C		NOT DESTROY X AND Y.	DRKGS065
C	OUTP	- THE NAME OF AN EXTERNAL OUTPUT SUBROUTINE USED.	DRKGS066
C		ITS PARAMETER LIST MUST BE X,Y,DERY,IHLF,NDIM,PRMT.	DRKGS067
C		NONE OF THESE PARAMETERS (EXCEPT, IF NECESSARY,	DRKGS068
C		PRMT(4),PRMT(5),...) SHOULD BE CHANGED BY	DRKGS069
C		SUBROUTINE OUTP. IF PRMT(5) IS CHANGED TO NON-ZERO,	DRKGS070
C		SUBROUTINE DRKGS IS TERMINATED.	DRKGS071
C	AUX	- DOUBLE PRECISION AUXILIARY STORAGE ARRAY WITH 8	DRKGS072
C		ROWS AND NDIM COLUMNS.	DRKGS073
C			DRKGS074
C	REMARKS		DRKGS075
C		THE PROCEDURE TERMINATES AND RETURNS TO CALLING PROGRAM, IF	DRKGS076
C	(1)	MORE THAN 10 BISECTIONS OF THE INITIAL INCREMENT ARE	DRKGS077
C		NECESSARY TO GET SATISFACTORY ACCURACY (ERROR MESSAGE	DRKGS078
C		IHLF=11),	DRKGS079
C	(2)	INITIAL INCREMENT IS EQUAL TO 0 OR HAS WRONG SIGN	DRKGS080
C		(ERROR MESSAGES IHLF=12 OR IHLF=13),	DRKGS081
C	(3)	THE WHOLE INTEGRATION INTERVAL IS WORKED THROUGH,	DRKGS082
C	(4)	SUBROUTINE OUTP HAS CHANGED PRMT(5) TO NON-ZERO.	DRKGS083
C			DRKGS084
C		SUBROUTINES AND FUNCTION SUBPROGRAMS REQUIRED	DRKGS085
C		THE EXTERNAL SUBROUTINES FCT(X,Y,DERY) AND	DRKGS086
C		OUTP(X,Y,DERY,IHLF,NDIM,PRMT) MUST BE FURNISHED BY THE USER.	DRKGS087
C			DRKGS088
C	METHOD		DRKGS089
C		EVALUATION IS DONE BY MEANS OF FOURTH ORDER RUNGE-KUTTA	DRKGS090
C		FORMULAE IN THE MODIFICATION DUE TO GILL. ACCURACY IS	DRKGS091
C		TESTED COMPARING THE RESULTS OF THE PROCEDURE WITH SINGLE	DRKGS092
C		AND DOUBLE INCREMENT.	DRKGS093
C		SUBROUTINE DRKGS AUTOMATICALLY ADJUSTS THE INCREMENT DURING	DRKGS094
C		THE WHOLE COMPUTATION BY HALVING OR DOUBLING. IF MORE THAN	DRKGS095
C		10 BISECTIONS OF THE INCREMENT ARE NECESSARY TO GET	DRKGS096
C		SATISFACTORY ACCURACY, THE SUBROUTINE RETURNS WITH	DRKGS097
C		ERROR MESSAGE IHLF=11 INTO MAIN PROGRAM.	DRKGS098
C		TO GET FULL FLEXIBILITY IN OUTPUT, AN OUTPUT SUBROUTINE	DRKGS099
C		MUST BE FURNISHED BY THE USER.	DRKGS100
C		FOR REFERENCE, SEE	DRKGS101
C		RALSTON/WILF, MATHEMATICAL METHODS FOR DIGITAL COMPUTERS,	DRKGS102
C		WILEY, NEW YORK/LONDON, 1960, PP.110-120.	DRKGS103
C			DRKGS104
C		.....	DRKGS105
C			DRKGS106
362		SUBROUTINE DRKGS(PRMT,Y,DERY,NDIM,IHLF,FCT,OUTP,AUX,ALT,X,	
		CTR, TI, MR, MI, R, CC, DCL, DCM, DCN, WHY, SS, ED, CF, OMEGA, ELECM, PERME, E, K,	
		C ZDATA)	
C			DRKGS108
C			DRKGS109
363		DIMENSION Y(8), DERY(8), AUX(8,8), A(8), B(8), C(8), PRMT(5), TR(4,4),	DRKGS110
		C TI(4,4), MR(3,3), MI(3,3), ED(119), CF(119), ALT(120), R(8)	DRKGS111
364		REAL*8 PRMT, Y, DERY, AUX, A, B, C, X, XEND, H, AJ, BJ, CJ,	DRKGS112
		C DELT, DABS, DCL, DCM, DCN, WHY, ED, CF, SS, CC,	
		COMEGA, PERME, E, ELECM, TR, TI, R1, R2, MR, MI, R, K, ALT, EVE, ZDATA	
365		EVE = 0.000	

366	DO 1 I=1,NDIM	DRKGS113
367	1 AUX(8,I)=.06666666666666667D0 *DERY(I)	DRKGS114
368	X=PRMT(1)	DRKGS115
369	XEND=PRMT(2)	DRKGS116
370	H=PRMT(3)	DRKGS117
371	PRMT(5)=0.D0	DRKGS118
372	CALL FCT(X,Y,DERY,TR,TI,MR,MI,SS,CC,DCL,DCM,DCN,ED,CF,OMEGA, DRKGS119 CELECM,PERME,E,K,ALT,PRMT,N,EVE,ZDATA)	
	C	DRKGS120
	C ERROR TEST	DRKGS121
373	IF(H*(XEND-X))38,37,2	DRKGS122
	C	DRKGS123
	C PREPARATIONS FOR RUNGE-KUTTA METHOD	DRKGS124
374	2 A(1)=.5D0	DRKGS125
375	A(2)=.2928932188134525D0	DRKGS126
376	A(3)=1.707106781186548D0	DRKGS127
377	A(4)=.16666666666666667D0	DRKGS128
378	B(1)=2.D0	DRKGS129
379	B(2)=1.D0	DRKGS130
380	B(3)=1.D0	DRKGS131
381	B(4)=2.D0	DRKGS132
382	C(1)=.5D0	DRKGS133
383	C(2)=.2928932188134525D0	DRKGS134
384	C(3)=1.707106781186548D0	DRKGS135
385	C(4)=.5D0	DRKGS136
	C	DRKGS137
	C PREPARATIONS OF FIRST RUNGE-KUTTA STEP	DRKGS138
386	DO 3 I=1,NDIM	DRKGS139
387	AUX(1,I)=Y(I)	DRKGS140
388	AUX(2,I)=DERY(I)	DRKGS141
389	AUX(3,I)=0.D0	DRKGS142
390	3 AUX(6,I)=0.D0	DRKGS143
391	I REC=0	DRKGS144
392	H=H+H	DRKGS145
393	IHLF=-1	DRKGS146
394	ISTEP=0	DRKGS147
395	IEND=0	DRKGS148
	C	DRKGS149
	C	DRKGS150
	C START OF A RUNGE-KUTTA STEP	DRKGS151
396	4 IF((X+H-XEND)*H)7,6,5	DRKGS152
397	5 H=XEND-X	DRKGS153
398	6 IEND=1	DRKGS154
	C	DRKGS155
	C RECORDING OF INITIAL VALUES OF THIS STEP	DRKGS156
399	7 IF(PRMT(5))40,8,40	DRKGS158
400	8 ITEST=0	DRKGS159
401	9 ISTEP=ISTEP+1	DRKGS160
	C	DRKGS161
	C	DRKGS162
	C START OF INNERMOST RUNGE-KUTTA LOOP	DRKGS163
402	J=1	DRKGS164
403	10 AJ=A(J)	DRKGS165
404	BJ=B(J)	DRKGS166
405	CJ=C(J)	DRKGS167
406	DO 11 I=1,NDIM	DRKGS168
407	R1=H*DERY(I)	DRKGS169
408	R2=AJ*(R1-BJ*AUX(6,I))	DRKGS170
409	Y(I)=Y(I)+R2	DRKGS171
410	R2=R2+R2+R2	DRKGS172
411	11 AUX(6,I)=AUX(6,I)+R2-CJ*R1	DRKGS173
412	IF(J-4)12,15,15	DRKGS174
413	12 J=J+1	DRKGS175
414	IF(J-3)13,14,13	DRKGS176
415	13 X=X+.5D0*H	DRKGS177
416	14 CALL FCT(X,Y,DERY,TR,TI,MR,MI,SS,CC,DCL,DCM,DCN,ED,CF,OMEGA, DRKGS178 CELECM,PERME,E,K,ALT,PRMT,N,EVE,ZDATA)	
417	GOTO 10	DRKGS179
	C	DRKGS180
	C	DRKGS181
	C	DRKGS182
	C TEST OF ACCURACY	DRKGS183
418	15 IF(ITEST)16,16,20	DRKGS184
	C	DRKGS185

	C	IN CASE ITEST=0 THERE IS NO POSSIBILITY FOR TESTING OF ACCURACY	DRKGS186
419	16	DO 17 I=1,NDIM	DRKGS187
420	17	AUX(4,I)=Y(I)	DRKGS188
421		ITEST=1	DRKGS189
422		ISTEP=ISTEP+ISTEP-2	DRKGS190
423	18	IHLF=IHLF+1	DRKGS191
424		X=X-H	DRKGS192
425		H=.500*H	DRKGS193
426		DO 19 I=1,NDIM	DRKGS194
427		Y(I)=AUX(1,I)	DRKGS195
428		DERY(I)=AUX(2,I)	DRKGS196
429	19	AUX(6,I)=AUX(3,I)	DRKGS197
430		GOTO 9	DRKGS198
	C		DRKGS199
	C	IN CASE ITEST=1 TESTING OF ACCURACY IS POSSIBLE	DRKGS200
431	20	IMOD=ISTEP/2	DRKGS201
432		IF(ISTEP-IMOD-IMOD)21,23,21	DRKGS202
433	21	CALL FCT(X,Y,DERY,TR,TI,MR,MI,SS,CC,DCL,DCM,DCN,ED,CF,OMEGA,CELECM,PERME,E,K,ALT,PRMT,N,EVE,ZDATA)	DRKGS203
434		DO 22 I=1,NDIM	DRKGS204
435		AUX(5,I)=Y(I)	DRKGS205
436	22	AUX(7,I)=DERY(I)	DRKGS206
437		GOTO 9	DRKGS207
	C		DRKGS208
	C	COMPUTATION OF TEST VALUE DELT	DRKGS209
438	23	DELT=0.00	DRKGS210
439		DO 24 I=1,NDIM	DRKGS211
440	24	DELT=DELT+AUX(8,I)*DABS(AUX(4,I)-Y(I))	DRKGS212
441		IF(DELT-PRMT(4))28,28,25	DRKGS213
	C		DRKGS214
	C	ERROR IS TOO GREAT	DRKGS215
442	25	IF(IHLF-20)26,36,36	DRKGS216
443		DO 27 I=1,NDIM	DRKGS217
444	27	AUX(4,I)=AUX(5,I)	DRKGS218
445		ISTEP=ISTEP+ISTEP-4	DRKGS219
446		X=X-H	DRKGS220
447		IEND=0	DRKGS221
448		GOTO 18	DRKGS222
	C		DRKGS223
	C	RESULT VALUES ARE GOOD	DRKGS224
449	28	CALL FCT(X,Y,DERY,TR,TI,MR,MI,SS,CC,DCL,DCM,DCN,ED,CF,OMEGA,CELECM,PERME,E,K,ALT,PRMT,N,EVE,ZDATA)	DRKGS225
450		DO 29 I=1,NDIM	DRKGS226
451		AUX(1,I)=Y(I)	DRKGS227
452		AUX(2,I)=DERY(I)	DRKGS228
453		AUX(3,I)=AUX(6,I)	DRKGS229
454		Y(I)=AUX(5,I)	DRKGS230
455	29	DERY(I)=AUX(7,I)	DRKGS231
456		IF(PRMT(5))40,30,40	DRKGS233
457	30	DO 31 I=1,NDIM	DRKGS234
458		Y(I)=AUX(1,I)	DRKGS235
459	31	DERY(I)=AUX(2,I)	DRKGS236
460		IREC=IHLF	DRKGS237
461		IF(IEND)32,32,39	DRKGS238
	C		DRKGS239
	C	INCREMENT GETS DOUBLED	DRKGS240
462	32	IHLF=IHLF-1	DRKGS241
463		ISTEP=ISTEP/2	DRKGS242
464		H=H+H	DRKGS243
465		IF(IHLF)4,33,33	DRKGS244
466	33	IMOD=ISTEP/2	DRKGS245
467		IF(ISTEP-IMOD-IMOD)4,34,4	DRKGS246
468	34	IF(DELT-.02DC*PRMT(4))35,35,4	DRKGS247
469	35	IHLF=IHLF-1	DRKGS248
470		ISTEP=ISTEP/2	DRKGS249
471		H=H+H	DRKGS250
472		GOTO 4	DRKGS251
	C		DRKGS252
	C	RETURNS TO CALLING PROGRAM	DRKGS253
473	36	IHLF=21	DRKGS255
474		CALL FCT(X,Y,DERY,TR,TI,MR,MI,SS,CC,DCL,DCM,DCN,ED,CF,OMEGA,CELECM,PERME,E,K,ALT,PRMT,N,EVE,ZDATA)	DRKGS256
475		GOTO 39	DRKGS257
476	37	IHLF=12	DRKGS258
477		GOTO 39	DRKGS259
478	38	IHLF=13	DRKGS260
479	39	CALL OUTP(X,Y,DERY,IHLF,NDIM,PRMT,N,R,CC)	DRKGS261
480	40	RETURN	DRKGS262
481		END	DRKGS263

\$ENTRY

UNITY  
1.00000000CCD CC

M(COMPLEX CALC.)

-3.9785399124D 02 -2.7967909108D 02 2.1216613366D 02 6.4698608386D 01 -1.2417872526D 03 -8.8191673325D 02  
2.1220968545D 02 2.3181439932D 02 -1.1160852567D 02 -7.9678289626D 01 6.6026055190D 02 4.3447874893D 02  
-1.2417798108D 03 -8.5336107163D 02 6.6027454799D 02 4.8818417536D 02 -3.8628583396D 03 -2.7006908802D 03

T(COMPLEX CALC.)

-1.95959D-01 1.60360D-03 -1.06761D-01 -2.81786D-03 -0.00000D-01 -0.00000D-01 1.00007D 00 -4.56837D-05  
-0.00000D-01 -0.00000D-01 -0.00000D-01 -0.00000D-01 1.00000D 00 0.00000D-01 0.00000D-01 0.00000D-01  
2.56529D-02 -9.46303D 01 2.02804D 00 -9.61541D-01 -0.00000D-01 -0.00000D-01 -1.02757D-01 2.90518D-03  
2.47780D 00 -9.61571D-01 8.42041D-02 9.46303D 01 0.00000D-01 0.00000D-01 -1.98088D-01 -1.43939D-03

BE

9.8511668580D-02 -4.1052340573D-05  
-7.4452278704D-01 3.2054206645D-01  
-6.1505255221D-02 2.5630818368D-05  
-8.9513429810D 03 1.5692306167D 00

FN

-1.0000000616D 00 1.1298477043D-08

Q

9.7435241374D 00 -4.9398453145D-02  
-9.9435380440D 00 5.1482942608D-02  
-1.4521257849D-01 9.6101521659D 00  
-4.8420189219D-02 -9.6120724460D 00

ZERO

1.0905157833D-03 -3.7385745080D-03  
1.0896860822D-03 -3.7416783549D-03  
1.1511382600D-03 3.3972853300D-03  
1.1492692111D-03 3.3994246232D-03

QUP

9.7435241374D 00 -4.9398453145D-02  
-4.8420189219D-02 -9.6120724460D 00

## INITIAL VALUE OF R

8.6910140192D-01	-1.2709250980D-01
1.0255621493D-01	8.2323240644D-02
1.0221290519D-01	7.8483021349D-02
-9.1803711576D-01	8.5317074115D-02

## INITIAL VALUE OF DERR

2.3378398674D-08	2.1103077460D-08
-1.5900082246D-05	1.8188395264D-05
1.5200690695D-05	-1.8139230186D-05
-8.5807963210D-09	-6.6649396075D-09

## STARTING REFLECTION COEFFICIENTS

MAGR

FAZR

8.7834483402D-01	-8.3196415161D 00
1.3150998442D-01	3.8754469178D 01
1.2886832410D-01	3.7518447210D 01
9.2199296692D-01	-5.3094848225D 00

## INITIAL VALUE OF Y

REALY

IMAGY

4.9049952455D 00	-4.8188981424D 00
4.8299810777D 00	-4.8948591669D 00
4.6283928767D 00	-4.8975146836D 00
-4.9859671542D 00	4.8436374827D 00

## INITIAL VALUE OF DERY

REALDERY

IMAGDERY

-1.7527735830D-17	6.3936400016D-17
8.6526744146D-04	9.2021673507D-04
-8.6198437341D-04	-8.8808565503D-04
5.0543953345D-07	-3.5497083304D-07



```

6.4750000000 04 0 -1.6482993321D-01 1.3666819054D-01 6.3875952753D-05 -2.1614137969D-03 4.4963581403D-01 -7.2691793566D-01
2.0819946549D 00 -7.8650709482D-02 -1.5410148799D-03 -4.6413627779D-04 8.4528582356D-01 -4.3174822275D-01
1.8325055974D 00 1.1771692887D-01 -1.3093142998D-03 -5.4515346748D-04 7.7984217674D-01 -3.0275843491D-01
4.5497244701D-01 -1.5454688800D 00 -6.7376783577D-04 2.3292883283D-03 -6.1987083388D-01 -1.2216063004D-01

```

118

X	IHLF N	REALY	IMAGY	REALDERY	IMAGDERY	REALR	IMAGR
6.4750000000	04 0	-1.6482993321D-01	1.3666819054D-01	6.3875952753D-05	-2.1614137969D-03	4.4963581403D-01	-7.2691793566D-01
		2.0819946549D 00	-7.8650709482D-02	-1.5410148799D-03	-4.6413627779D-04	8.4528582356D-01	-4.3174822275D-01
		1.8325055974D 00	1.1771692887D-01	-1.3093142998D-03	-5.4515346748D-04	7.7984217674D-01	-3.0275843491D-01
		4.5497244701D-01	-1.5454688800D 00	-6.7376783577D-04	2.3292883283D-03	-6.1987083388D-01	-1.2216063004D-01

FINAL REFLECTICN COEFFICIENT VALUES

	MAGR	FAZR
11R11	8.5474092591D-01	3.2826108915D 02
11R +	9.4916523923D-01	2.9705666408D 02
+ R11	8.3655035146D-01	2.9121772322D 02
+ R +	6.3179353449D-01	1.9114865971D 02

COMPILE TIME= 3.14 SEC, EXECUTION TIME= 145.85 SEC, OBJECT CODE= 51120 BYTES, ARRAY AREA= 5728 BYTES, UNUSED= 243152 BYTES

\$STOP

## REFERENCES

- Aikin, A. C., J. A. Kane and J. Troim (1964), Some results of rocket experiments in the quiet D region, *J. Geophys. Res.* 69, 4621-4628.
- Bain, W. C. and B. R. May (1967), D region electron-density distributions from propagation data, *Proc. Instn. Elect. Engrs.* 114, 1593-1597.
- Barron, D. W. and K. G. Budden (1959), The numerical solution of differential equations governing the reflexion of long radio waves from the ionosphere III, *Proc. Roy. Soc.* A249, 387-401.
- Belrose, J. S. and I. A. Bourne (1966), The electron distribution and collision frequency height profile for the lower part of the ionosphere (the D and lower E regions), Ground-based Radio Wave Propagation Studies of the Lower Ionosphere, Conference Proceedings, 1, 79-96.
- Booker, H. G. (1938), Propagation of wave-packets incident obliquely upon a stratified doubly refracting ionosphere, *Phil. Trans.* A237, 411-450.
- Bracewell, R. N. (1952), The ionospheric propagation of radio waves of frequency 16 kc/s over distances of about 200 km, *Proc. Instn. Elect. Engrs.* 99-IV, 217-228.
- Budden, K. G. (1955a), The numerical solution of differential equations governing reflexion of long radio waves from the ionosphere I, *Proc. Roy. Soc.* A227, 516-537.
- Budden, K. G. (1955b), The numerical solution of the differential equations governing the reflexion of long radio waves from the ionosphere II, *Phil. Trans.* A248, 45-71.
- Budden, K. G. (1961), Radio Waves in the Ionosphere, Cambridge University Press.
- Burnside, W. S. and A. W. Panton (1904), The Theory of Equations, Dublin University Press, Dublin, Ireland.
- Crombie, D. D. (1961), Reflection from a sharply bounded ionosphere for VLF propagation perpendicular to the magnetic meridian, *J. Res. NBS* 65D, 455-463.
- Deeks, D. G. (1964), Some tentative suggestions of electron density profiles in the D region, Internal Memorandum No. 121, Radio and Space Research Station, Slough, England.
- Deeks, D. G. (1966a), Generalised full wave theory for energy-dependent collision frequencies, *J. Atmosph. Terr. Phys.* 28, 839-846.
- Deeks, D. G. (1966b), D-region electron distributions in middle latitudes deduced from the reflexion of long radio waves, *Proc. Roy. Soc.* 291, 413-437.

- Farley, D. T. (1966), Observations of the equatorial ionosphere using incoherent backscatter, Electron Density Profiles in Ionosphere and Exosphere, North-Holland Publishing Co., Amsterdam, 446-477.
- Fedor, J., L. Fedor and E. E. Gossard (1964), Program for the full-wave calculation of reflection coefficients in an ionosphere continuous in electron density and collision frequency, Interim Report, U. S. Navy Electronics Laboratory, San Diego, California.
- Fejer, J. A. and R. W. Vice (1959), An investigation of the ionospheric D-region, *J. Atmosph. Terr. Phys.* 16, 291-306.
- Gill, S. (1951), A process for the step-by-step integration of differential equations in an automatic digital computing machine, *Proc. Camb. Phil. Soc.* 47, 96-108.
- Heading, J. and R. T. P. Whipple (1952), The oblique reflexion of long wireless waves from the ionosphere at places where the earth's magnetic field is regarded as vertical, *Phil. Trans.* A244, 469-503.
- Hunten, D. M. and M. B. McElroy (1968), Metastable  $O_2(^1\Delta)$  as a major source of ions in the D region, *J. Geophys. Res.* 73, 2421-2428.
- McCracken, D. D. (1965), A Guide to Fortran IV Programming, John Wiley and Sons, Inc.
- Mechtly, E. A. and L. G. Smith (1968), Seasonal variation of the lower ionosphere at Wallops Island during the IQSY, *J. Atmosph. Terr. Phys.* 30, 1555-1561.
- Monro, P. E. and S. A. Bowhill (1969), Minor atmospheric constituents and the ion composition of the E-region, *J. Atmosph. Terr. Phys.* 31, 103-117.
- Nicolet, M. and A. C. Aikin (1960), The formation of the D region of the ionosphere, *J. Geophys. Res.* 65, 1469-1483.
- Pitteway, M. L. V. (1965), The numerical calculation of wave-fields, reflexion coefficients and polarizations for long radio waves in the lower ionosphere I, *Phil. Trans.* A257, 219-242.
- Sechrist, C. F., Jr. (1968), Interpretation of the pre-sunrise electron densities and negative ions in the D-region, *J. Atmosph. Terr. Phys.* 30, 371-389.
- Sen, H. K. and A. A. Wyller (1960), On the generalization of the Appleton-Hartree magnetoionic formulas, *J. Geophys. Res.* 65, 3931-3950.
- Sheddy, C. H. (1963), A general analytic solution for reflection from a sharply bounded ionosphere, *Radio Science* 3, 792-795.

- Smith, R. A., T. N. R. Coyne, R. G. Loch and I. A. Bourne (1966), Small perturbation wave interaction in the lower ionosphere, Part 3, Ground-based Radio Wave Propagation Studies of the Lower Ionosphere, Conference Proceedings, 1, 335-358.
- Tulinov, V. F. (1967), On the role of corpuscular radiation in the formation of the lower ionosphere (below 100 km), Space Research VII, Vol. 2, 386-390.
- Velinov, P. (1968), On ionization in the ionospheric D-region by galactic and solar cosmic rays, J. Atmosph. Terr. Phys. 30, 1891-1905.